Optimal cross-border electricity trading

Álvaro Cartea* Maria Flora † Tiziano Vargiolu ‡ Georgi Slavov§

December 15, 2021

Abstract

We show there exists a profitable cross-border trading strategy for an agent who trades electricity in the European electricity network. Data of the European markets are employed to show how electricity prices in all locations of the network are affected by the flow of power between any two locations that trade power between them. The optimal cross-border trading strategy is derived via the explicit solution of a non-trivial stochastic control problem in which prices at different locations are co-integrated and trading affects prices in all locations of the network.

Keywords: stochastic optimal control, electricity interconnector, co-integration, cross-border price impact, electricity network.

1 Introduction

The market coupling initiatives in the European Union seek to integrate the European wholesale electricity markets to increase security of supply and to make the day-ahead and intraday power markets more efficient.[1] At the core of these initiatives, is to extend the European power network by investing in bi-directional transmission lines (i.e., interconnectors) to link the electricity grids of pairs of countries.

In this paper, we develop a model of cross-border intraday trading for an agent who trades electricity in a collection of pairs of countries that are part of a power network. That is, the

*University of Oxford, Mathematical Institute - Oxford-Man Institute of Quantitative Finance, Oxford, UK - alvaro.cartea@maths.ox.ac.uk

†CREST, CNRS, Institut Polytechnique de Paris, France - maria.flora@ensae.fr

‡Università degli Studi di Padova, Department of Mathematics, Italy - vargiolu@math.unipd.it

§Marex Spectron Ltd, London, UK

[1]See for example, Newbery et al. (2016) and www.eirgridgroup.com/customer-and-industry/european-integration/.

agent purchases electricity in one location and sells it in another location and the electricity is transmitted via the interconnector that links the two locations.

We show that transmission of electricity across borders has a direct effect on the prices of power in the two locations that import and export the electricity, and may have an indirect effect on the prices of power in other locations of the network. In both cases, prices are affected because the transactions alter the demand and supply of power in the locations of the network. We refer to the direct and indirect effects on the prices of power as permanent price impact.

In our model, the agent maximises expected profits from cross-border trading of power during a finite-time horizon. The optimal trading strategy accounts for the permanent price impact of the trades and also accounts for the temporary price impact. The latter refers to the difference between the best price the agent observes at the time she trades and the price she achieves. In general, when the agent buys (resp. sells) power, the average execution price she pays (resp. receives) per megawatt (MW) is higher (resp. lower) than the best quote in the market at the time of the transaction. This temporary price impact is a result of the limited liquidity at the best quotes in the market. We label the effect as temporary because we assume that liquidity replenishes immediately after a trade is executed.

We show that the agent's optimal cross-border trading strategy for each pair of interconnected locations consists of the sum of two terms. The first term is a function of the difference between the prices in two interconnected locations and the costs due to: temporary price impact of the trades, interconnector costs, and exchange fees. When the prices in the two locations are different, the agent purchases power in the location with lower price and sells the power in the other location. The amount of electricity that can be traded at a profit is capped by: temporary price impact, interconnector costs, and exchange fees. If there were no trading costs and the temporary price impacts were zero (i.e., infinite liquidity) the strategy would be to purchase an infinite amount of power in the location with lower price and sell it in the location with higher price – however, a transaction of a very large amount of power is not possible because the two markets cannot bear those volumes at the marginal prices that are quoted.

The other term of the optimal strategy is a function of the permanent price impact, direct and indirect, of the agent's trading activity and of interconnector costs, and exchange fees. Purchasing (selling) electricity in one location exerts an upward (a downward) pressure on the prices of power in that location, and possibly in other locations of the network. The magnitude of the price pressure is proportional to the quantity of power bought and sold.

In our study, we employ data of the power transmitted via the interconnectors between France, Germany, Switzerland, Austria, Belgium, the Netherlands, and Luxembourg, and use price data from the European Power Exchange (EPEX). We estimate the direct and indirect permanent price impacts that electricity flows in these European countries have on the prices of electricity in France, Germany, and Switzerland. To the best of our knowledge, this is the first paper that employs interconnector flows to estimate price impact in the various locations of the network. Our results show that there are both direct and indirect permanent price impacts. For example, for contracts that deliver electricity during the hour that ends at 2pm, power flows from Switzerland to Germany have a direct permanent impact on electricity prices in both Switzerland and Germany, and also have an indirect permanent price impact on the price of power in France. Similarly, power flows from Switzerland to France have a direct permanent impact on electricity prices in both Switzerland and France, and also have an indirect permanent price impact on the price of power in Germany. Moreover, the permanent price impacts are not symmetric. That is, all else being equal, the permanent price impact due to exporting power from country j into country i is, for most of the contracts we study, different from the price impact of a transaction to export power from country i into country j.

We analyse the performance of the strategy for a range of interconnector costs and exchange fees when the agent trades power between France, Switzerland, and Germany. If interconnection costs and exchange fees are zero, the yearly profit is approximately €130 million per calendar year and the strategy trades an average of 294 million MWh. As costs increase, trading activity and profits decrease. For example, when the costs of employing the interconnector and exchange fees are the same as those that stem from the temporary price impact of the trades, the yearly average profit decreases to €57 million and the strategy trades an average of 130 million MWh.

Previous work on interconnectors in the energy market includes that by Cartea and González-Pedraz (2012). The authors employ a static trading strategy (not dynamically optimal) to value an interconnector as a strip of options written on the spread between power prices in two countries and derive no-arbitrage lower bounds for the value of the interconnector. They cap the profits of the strategy to account for the liquidity constraints in the power market. However, in our paper, the liquidity constraints are determined by the temporary price impact, interconnector costs, and exchange fees and, more importantly, the decisions to trade are dynamically optimal and account for permanent price impacts.

In regard to the broader value and use of interconnectors in power markets, the work of

McInerney and Bunn (2013) examines the Irish and British electricity markets and find that auction prices for transmission rights are undervalued against spread option valuations. The work of Newbery et al. (2016) finds that the potential value of coupling interconnectors to increase the efficiency of trading day-ahead, intraday, and balancing services across borders in the EU is approximately €3.9 billion per year. Moreover, Kiesel and Kusterman (2016) study the effect of market coupling on the dynamics and on distribution of electricity prices, and on the value of power plants, for which they propose a multi-market framework.

Our work is closest to that of Cartea et al. (2019), in which the authors derive an optimal strategy (robust to model misspecification) to trade electricity contracts in two locations that are joined by an interconnector, and the contracts are not for physical delivery of power. Our approach is different in various ways. First, we employ electricity flows and transactions data in the European power network to determine the indirect and direct price impact of trades. Second, in our model, the agent trades in various locations of the power network (instead of only two locations) and the contracts are for physical delivery of power. Third, we derive the optimal cross-border trading strategy in closed-form for a power network with a finite number of interconnected locations.

Our framework can also be used to derive optimal trading strategies for cross-listed stocks in different venues. The literature related to this topic includes the work of Mudchanatongsuk et al. (2008), which models the difference of the log-prices of a pair of co-integrated stocks and employs stochastic control techniques to derive an optimal trading strategy; Tourin and Yan (2013) employ a similar co-integration model and find a closed-form solution for a dynamic trading strategy that takes positions in a risk-free bond and in two stocks – for extensions to this model see Leung and Li (2015) and Lei and Xu (2015), where the authors formulate an optimal entry-exit strategy on a pair of co-integrated assets. Finally, Cartea and Jaimungal (2016a) and Lintilhac and Tourin (2017) generalise the results in Tourin and Yan (2013) to include an arbitrary number of assets.

The remainder of the paper is organised as follows. Section 2 discusses the data we employ. Section 3 presents the model and derives the optimal strategy for cross-border trading. Section 4 presents the econometric analysis to estimate the direct and indirect effects of cross-border flows on electricity prices and estimates the model parameters. Section 5 illustrates the performance of the cross-border strategy and Section 6 concludes. We collect part of the proofs and supplementary tables in the appendix.

2 The European Power Exchange

Electricity is a commodity that cannot be stored or is too expensive to store. Thus, market participants trade contracts written on electricity, yet to be produced, for delivery in the future at a pre-specified time, location, and number of MWs, which are dispatched over a delivery period specified in the contract. For example, in the day-ahead market, electricity is traded approximately one day in advance and the delivery period of these contracts is within the following day. There are also intraday markets where delivery of power is in the same day the contract is traded, and there are other electricity markets where the delivery period is long into the future: weeks, months, quarters, and years.

Power can be traded as over-the-counter bilateral agreements and on exchanges. In Europe, one of the largest power exchanges is EPEX SPOT, which covers France, Germany, Switzerland, the United Kingdom, the Netherlands, Belgium, Austria, and Luxembourg. The EPEX SPOT operates two intraday markets. One is the EPEX SPOT Intraday Continuous, which is an intraday market with continuous trading – contracts can be traded up to minutes before physical fulfillment. The other is an intraday market that consists of a uniform price auction system.

In this paper we employ transaction-by-transaction data for all contracts with delivery period of hours and blocks of hours traded on EPEX Spot Intraday Continuous for the period 01/01/2016 to 31/12/2017. These contracts are traded in a limit order book and our data set consists of 7,306,380 transactions – Table 1 shows a few transactions for a day in March 2017. For each transaction, the table reports the hour and day of delivery, time when the transaction was executed, the locations that export and import the power, volume in MW, and the price in Euros per MWh.

In Table 1 we highlight a transaction that occurred at 11:05:00am on 5 March 2017 for delivery of 5MW on the same day during hour 9pm (i.e., 5MW will be delivered between 8pm and 9pm). The electricity will be exported from France and imported into Germany.

For each electricity contract, every day, the amount of electricity that can be imported from and exported to the interconnected locations is restricted by the available transfer capacity (ATC). As interconnector capacity is committed throughout the day, there is a reduction in the transfer capability of the physical transmission network. In each interconnected location, the transmission capacity is capped by the ATC. When this maximum capacity is reached, the relevant side of the order book closes until either offsetting orders are received and transmission

Delivery	Time Stamp	Location Buy	Location Sell	Volume MW	Price €/MWh
05/03/2017 h 9pm	05/03/2017 10:00:00 am	FR	AT	12	35.70
05/03/2017 h 9pm	05/03/2017 10:02:00 am	FR	AT	1	35.70
05/03/2017 h 9pm	05/03/2017 10:04:00 am	CH	DE	1	39.00
05/03/2017 h 9pm	05/03/2017 10:04:00 am	CH	AT	1	39.00
05/03/2017 h 9pm	05/03/2017 10:06:00 am	CH	DE	1	38.80
05/03/2017 h 9pm	05/03/2017 10:08:00 am	DE	DE	1	38.80
05/03/2017 h 9pm	05/03/2017 10:08:00 am	DE	AT	19	39.00
05/03/2017 h 9pm	05/03/2017 10:14:00 am	DE	CH	6	35.90
05/03/2017 h 9pm	05/03/2017 10:35:00 am	NL	AT	20	38.90
05/03/2017 h 9pm	05/03/2017 10:35:00 am	NL	DE	25	39.00
05/03/2017 h 9 pm	05/03/2017 11:05:00 am	FR	DE	5	37.10
05/03/2017 h 9 pm	05/03/2017 11:05:00 am	DE	DE	6	37.00
05/03/2017 h 9 pm	05/03/2017 11:17:00 am	NL	FR	1	38.00
05/03/2017 h 9 pm	05/03/2017 11:48:00 am	DE	DE	18	38.90
05/03/2017 h 9 pm	05/03/2017 12:02:00 pm	DE	AT	11	38.30
05/03/2017 h 9 pm	05/03/2017 12:02:00 pm	DE	AT	2	38.20
05/03/2017 h 9 pm	05/03/2017 12:02:00 pm	DE	AT	10	38.10

Table 1: Each row represents a trade in the intraday spot market and provides information about (from left to right) the hour and day of delivery, time of execution of the transaction, location where power is sourced and where it is dispatched, volume in MW, and price in Euros per MWh.

capacity is released back into the market, or a new trading day starts and the book is open for trades in the directions where there is available transmission capacity. Table 2 shows the ATC for various countries in the European power network. The ATC is lower than the net transfer capacity (NTC) because one needs to account for the committed import and export volumes under long term contracts (CVLT), and the transmission reliability margin (TRM),[2] hence

$$\text{ATC} = \text{NTC} - \text{CVLT} - \text{TRM}\,.$$

From	To	ATC (MW)
France	Switzerland	3,200
France	Germany	3,000
Germany	France	3,050
Germany	Switzerland	800
Switzerland	France	2,200
Switzerland	Germany	4,000

Table 2: ATC for power flows in each direction between two countries. Source: Marex Spectron Ltd.

We focus on cross-border trades among three countries in the EPEX: France, Germany, and Switzerland. In Table 3, the rows labeled 'all hours' report summary statistics of cross-border volumes of electricity traded in the intraday market for power delivered during all hours.[3]

[2]TRM refers to the amount of transmission transfer capacity that is set aside as a buffer to ensure the reliability of the system operation should conditions change.

[3]For example, we employ the volumes of the transactions in our data set where Location Buy = FR and Location Sell = CH to compute the statistics in the first row in Table 3 – the other statistics are computed in a

Observe that France is the country with the largest imports of power and Germany is the largest exporter of power. Throughout this paper, we hyphenate the names of pairs of countries to denote transmission flows: the first country in the pair exports the electricity and the other country in the pair imports the electricity, e.g., FR-CH denotes exports from France that are imported into Switzerland.

		Mean	Std. Dev.	Max	Min	Skewness	Kurtosis	# transac.
FR-CH	all hours	15.57	10.26	141	0.10	0.90	8.27	70,381
	11am	16.11	10.74	100	0.10	1.2	9.37	3,249
CH-FR	all hours	15.41	10.44	240	0.10	1.45	18.90	59,868
	11am	15.95	10.03	75	0.10	0.40	3.99	2,879
FR-DE	all hours	10.27	9.55	252.5	0.10	1.88	17.76	162,668
	11am	10.74	9.81	161.9	0.10	1.79	16.01	5,119
DE-FR	all hours	11.14	10.01	400	0.10	3.31	71.54	201,601
	11am	11.39	9.55	91.5	0.10	1.03	5.42	6,741
CH-DE	all hours	9.93	8.93	148.3	0.10	1.22	7.03	128,857
	11am	10.56	8.78	65	0.10	0.75	3.11	5,574
DE-CH	all hours	10.20	8.93	265	0.10	1.64	17.16	157,004
	11am	11.05	8.84	75	0.10	0.77	3.61	7,369

Table 3: Imports and exports of electricity. Descriptive statistics of the cross-border volumes exchanged between France, Germany, and Switzerland for all cross-border intraday contracts (rows 'all hours') and for contracts with delivery during a peak (11am) hour (rows '11am'). The values of mean, standard deviation, maximum, and minimum are expressed in MWh.

The rows labeled '11am' in Table 3 present descriptive statistics for contracts that deliver electricity on hour 11am (i.e., from 10am to 11am), which is an on-peak hour.[4] For this hour, the trading direction with most cross-border activity is from Germany to Switzerland.[5] However, the contracts with the highest mean volume are for electricity exported from France into Switzerland.

Table 4 shows descriptive statistics of the prices of all 'internal' intraday hourly contracts traded in the three countries. Here, internal contracts refers to transactions where electricity is produced and dispatched within the same country, i.e., we exclude exports and imports. Internal transactions represent 78% of the total number of transactions in the data. For example, in Table 1 the transactions in rows 6, 12, and 14 are for power produced and dispatched within

similar way.

[4]To compute the values in the second row in Table 3 we employ the volumes of the transactions in the data set where Location Buy = FR and Location Sell = CH and Delivery = 11am. We follow a similar approach to compute the other values in the '11am' rows of the table.

[5]Total flows are computed as the product of the mean value of MW and the number of transactions. For example, for DE-CH hour 11am, the value is computed as $11.05\text{MW} \times 7,369$.

Germany. The country with the highest average price is Switzerland and it is also a net importer of power (i.e., imports more power from France and Germany than it exports to those two countries). Germany is the country with the largest number of internal transactions, and with the lowest average price. In addition, the results of the Augmented Dickey-Fuller (ADF) test on prices show that the unit root hypothesis is rejected, thus favouring a model in which prices mean revert to a seasonal level. The Jarque-Bera tests suggest that prices are not normally distributed. The same results, both for the ADF test and the Jarque-Bera, hold for all single peak and off-peak hours.

	France	Switzerland	Germany
Mean	48.13	49.51	32.78
Std. Dev.	36.57	42.75	17.44
Max	1600.00	1300.00	650.00
Min	−37.20	−120.00	−320.00
Skewness	15.03	12.76	1.43
Kurtosis	388.35	266.14	32.38
ADF	0.01%	0.01%	0.01%
Jarque-Bera	0.01%	0.01%	0.01%
# of trans.	187,785	45,455	5,487,663

Table 4: Internal transactions for all hours. Descriptive statistics of the prices for all internal intraday contracts traded among France, Germany, and Switzerland. The values for mean, standard deviation, maximum, and minimum are expressed in €/MW. We report the p-values of the Augmented Dickey-Fuller (ADF) test statistic, which indicate that the null hypothesis of unit root is rejected in favor of the mean reverting alternative in all cases. We also report the p-values for the Jarque-Bera test, which reject, in all cases, the null hypothesis of normality.

Table 5 shows descriptive statistics of the price for internal contracts with delivery on hour 11am. On average, depending on interconnector costs and exchange fees, it may be profitable to export electricity for the 11am hourly slot from Germany to both Switzerland and France.

	France	Switzerland	Germany
Mean	50.31	68.73	35.68
Std. Dev.	22.68	127.06	17.11
Max	350.00	1300.00	300.00
Min	0.00	−2.00	−85.00
Skewness	1.97	6.82	2.11
Kurtosis	11.83	50.82	25.91
ADF	0.01%	0.01%	0.01%
Jarque-Bera	0.01%	0.01%	0.01%
# of trans.	9,128	2,213	265,744

Table 5: Internal transactions for hour 11am. The values for mean, standard deviation, maximum and minimum are expressed in €/MW. We report the p-values of the Augmented Dickey-Fuller (ADF) test statistic, which indicate that the null hypothesis of unit root is rejected in favor of the mean reverting alternative in all cases. We also report the p-values for the Jarque-Bera test, which reject in all cases, the null hypothesis of normality.

3 The model

In this section, we propose a model for cross-border trading of electricity in n locations. The novelty of our approach is the explicit inclusion of cross-border impacts in the electricity price dynamics. Also, we model co-movements in prices of power in a network of interconnected locations, and we take into account the peculiar features of the dynamics of electricity prices, such as large spikes and quick reversion to a seasonal level. The literature on modelling power prices is vast, see for example Roncoroni (2002), Cartea and Figueroa (2005), Benth et al. (2007), Weron (2007), Borak and Weron (2008), Hambly et al. (2009), Kiesel et al. (2009), Cartea et al. (2009), Gianfreda and Bunn (2018), Kiesel et al. (2019), and Ronn and Wimschulte (2009) – see also Benth et al. (2012) for a critical comparison of the first three models.

Denote by $\Theta_k(t)$ the seasonal level of power prices in country k and specify it as follows:

$$\Theta_k(t) = b_{1,k}\,\sin(2\,\pi\,t) + b_{2,k}\,\cos(2\,\pi\,t) + b_{3,k}\,\sin(4\,\pi\,t) + b_{4,k}\,\cos(4\,\pi\,t) + b_{5,k}\,t + b_{6,k}\,, \qquad (3.1)$$

where we model the annual (period $2\,\pi$) and the semi-annual (period $4\,\pi$) seasonality with different centers, see Lucia and Schwartz (2002), Seifert and Uhrig-Homburg (2007), and Pilipovic (1998). We define the midprice of electricity as $\widetilde{P}_t^k = P_t^k + \Theta_k(t)$, where P_t^k is the de-seasonalised electricity midprice in country k and t denotes time. From now on, for simplicity, we also refer to P_t^k as the price of electricity.

We denote by $\boldsymbol{P}_t^{\boldsymbol{\nu}}$ the vector of prices and assume it follows the dynamics

$$\mathrm{d}\mathbf{P}_t^{\boldsymbol{\nu}} = (\boldsymbol{\theta} - \boldsymbol{\Phi}\,\mathbf{P}_t^{\boldsymbol{\nu}} + \mathbf{g}(\boldsymbol{\nu}_t))\,\mathrm{d}t + \boldsymbol{\sigma}\,\mathrm{d}\mathbf{W}_t + J(\boldsymbol{\psi},\boldsymbol{\xi})\,\mathrm{d}\boldsymbol{\Pi}_t(\boldsymbol{\lambda})\,. \qquad (3.2)$$

The last two terms on the right-hand side of (3.2) represent the innovations in the price of electricity. The diffusive term $\boldsymbol{\sigma}\,\mathrm{d}\mathbf{W}_t$ represents shocks to prices in all countries where $(W_t^i)_{t>0}$ $i = 1, \cdots, n$ is a vector of standard Brownian motions independent of each other and $\boldsymbol{\sigma}$ is the Cholesky decomposition of the instantaneous variance-covariance matrix of electricity prices. The term $J(\psi_k, \xi_k)\,\mathrm{d}\Pi_t^k(\lambda_k)$ represents price spikes specific to each country, which arrive as a Poisson process Π_t^k with intensity λ_k and jump sizes are i.i.d. normally distributed with mean ψ_k and standard deviation ξ_k. The Poisson jumps are all independent of each other and independent of the Brownian motions.[6]

[6]Note that we assume that jumps are independent across countries. This is a simplifying assumption because jumps may be correlated across the countries in the power network. For example, jumps due to a sudden increase

The drift term in (3.2) has three components. The first is an idiosyncratic component represented by the constant vector $\boldsymbol{\theta}$, which affects the price in each country. The second is $\boldsymbol{\Phi}\,\mathbf{P}_t^{\boldsymbol{\nu}}$, and for each each country k we have

$$(\boldsymbol{\Phi}\,\mathbf{P}_t^{\boldsymbol{\nu}})^k = -\sum_{i=1}^{n} \delta_{ki}\,\alpha_t^i\,, \tag{3.3}$$

where $\sum_{i=1}^{n} \delta_{ki}\,\alpha_t^i$ is a proxy for all the drivers that cause co-movements in the prices of power in all locations. Here, the parameters δ_{ki} are country-specific constants, and

$$\alpha_t^i = \sum_{j=1}^{n} a_{ij}\,P_t^j \tag{3.4}$$

is the co-integration factor for country i, where a_{ij} are constants and n represents the number of countries in the network. Thus, the price of electricity in each country depends on the price of electricity in other countries of the power network.

In matrix form, we write $\boldsymbol{\Phi} = -\boldsymbol{\Delta}\,\mathbf{A}$, where

$$\boldsymbol{\Delta} = \begin{pmatrix} \delta_{11} & \cdots & \delta_{1n} \\ \vdots & \ddots & \vdots \\ \delta_{n1} & \cdots & \delta_{nn} \end{pmatrix} \qquad \text{and} \qquad \mathbf{A} = \begin{pmatrix} a_{11} & \cdots & a_{1n} \\ \vdots & \ddots & \vdots \\ a_{n1} & \cdots & a_{nn} \end{pmatrix}.$$

The third component of the drift is the permanent price impact function $\mathbf{g}(\boldsymbol{\nu}_t)$, where each element of the vector $\boldsymbol{\nu}_t$ denotes the cross-border activity between two locations. When the speed of trading ν^{ij} is positive, the agent buys the quantity $\nu^{ij}\Delta t$ MW of electricity in country i, and sells the same quantity in country j. Similarly, when ν^{ij} is negative, the agent buys the quantity $\nu^{ij}\Delta t$ MW of electricity in country j and simultaneously sells the same amount of electricity in country i. Thus, the agent's net position in electricity is always zero because the electricity bought in one location is immediately sold in another location.

We assume that the permanent price impact function $g(\boldsymbol{\nu}_t)$ is linear in the agent's speed of trading $\boldsymbol{\nu}_t$, and that it has the form

$$\mathbf{g}(\boldsymbol{\nu}_t) = \boldsymbol{H}\,\boldsymbol{\nu}_t\,, \tag{3.5}$$

in demand, caused by a cold snap, would affect neighbouring countries. In principle, we could include this in our model by assuming that the intensities in the jump processes have a common component and an idiosyncratic component. However, for simplicity, and to keep the model parsimonious, we assume that the Poisson processes are independent.

where $\boldsymbol{H}$ is a matrix of permanent price impact parameters.

We adopt two specifications of $\boldsymbol{H}\,\boldsymbol{\nu}_t$ that depend on whether the impact of the speeds of trading ν^{ij} on the prices in locations i and j is the same as or different from the impact of the speed ν^{ji} on the prices in locations j and i.

When the permanent price impacts are the same in both directions of the cross-border trade, which we refer to as the *constrained case*, we have

$$\boldsymbol{\nu} = (\boldsymbol{\nu}_t)_{\{0\leq t\leq T\}} = \left((\nu^{ij})_{i,j=1,\ldots,n,\, i<j}\right)_{\{0\leq t\leq T\}} \in \mathbb{R}^{n\,(n-1)/2}\,,$$

or in longhand notation,

$$\boldsymbol{\nu} = \left(\nu^{12},\, \nu^{13},\ldots,\, \nu^{1n},\, \nu^{23},\ldots,\, \nu^{2n},\ldots,\nu^{(n-1)n}\right)^{\mathsf{T}}\,, \tag{3.6}$$

and $\boldsymbol{H}$ is an $n \times n\,(n-1)/2$ matrix of cross-border price impacts. On the other hand, when the impacts are different in each direction, which we refer to as the *unconstrained case*, we have $\boldsymbol{\nu}_t \in \mathbb{R}^{n\,(n-1)}$, because the trading speed vector contains two speeds for each pair of locations, and $\boldsymbol{H}$ is an $n \times n\,(n-1)$ matrix.

In the following section we provide empirical support for both specifications, and later we solve the agent's cross-border problem in closed-form in the constrained case, i.e., when the permanent price impact of exporting power from location i to location j is the same as the price impact from exporting power from location j to location i.[7]

3.1 Temporary price impact

Due to limited liquidity (i.e., limited production capacity) at the best prices quoted in the market, orders sent by agents may be executed at worse prices than those quoted in the exchange by other market participants. For example, when a trader purchases power in one location, as the volume of the transaction increases, power becomes more expensive because the marginal

[7]Ideally, the agent would impose an upper and a lower bound on the speed of trading, so that $\nu_t^{ij} \in [L^{ij}, U_t^{ij}]$ with $L^{ij} = 0$ and $U_t^{ij} = \mathrm{atc}_t^{ij}$, where $\mathrm{atc}_t^{ij} \leq \mathrm{ATC}^{ij}$ denotes the residual transfer capacity at time t on the ij side of the order book. (recall that ATC denotes the maximum available transfer capacity of the interconnector, see Table 2). The restriction $L = 0$, i.e., that the speed cannot be negative, would be important to model the impact of imports and of exports on the electricity prices when these cross-border price impact parameters are different in each trading direction (unconstrained cross-border impacts). The assumption $-L^{ij} = U^{ij} = \infty$ for all pairs $i \neq j$, and thus the assumption of symmetric (constrained) cross-border price impacts, allows us to solve the investor's cross-border problem explicitly, i.e., to obtain the optimal cross-border trading speed and the value function in closed-form. In this unrestricted case, we have that $\nu_t^{ij} = -\nu_t^{ji}$ for all pairs of locations $i \neq j$ and for all t.

cost to produce electricity increases. Therefore, everything else being equal, the average price received by the order tends to worsen as the size of the order increases. We assume that this execution price impact is temporary, i.e., the liquidity in the market is quickly replenished, and we include the temporary price impact in the model as follows. Let the $1 \times n$ vector $\boldsymbol{\omega}$ denote the temporary price impact parameters with entries $\omega_k \geq 0$, for each location $k \in \{1, \cdots, n\}$. Then, the agent's execution price is given by

$$\widehat{P}_t^k = \widetilde{P}_t^k \pm \omega_k \, \nu_t^{kj} \tag{3.7}$$

when buying/selling $(+/-)$ in location k and selling/buying in location j, $j \neq k$.

Also, note that a transaction between two locations may have an instantaneous effect on other contracts traded in the power network because production capacity offered in one location was also simultaneously offered in other locations of the network. For example, when a trader purchases power in France to export it to Switzerland, the contracts for export/import between France and Germany are affected because French production capacity was concurrently offered in Germany and Switzerland (and other locations interconnected to the French power network). In this case, the agent's execution price is given by

$$\widehat{P}_t^k = \widetilde{P}_t^k \pm \sum_j \omega_k \, \nu_t^{kj} \, . \tag{3.8}$$

Recall that $\widetilde{P}_t^k$ denotes the midprice at time t before deseasonalisation, i.e., $\widetilde{P}_t^k = P_t + \Theta_k(t)$, with $\Theta(t)$ as in (3.1), which is the price the agent observes before trading, and note that (3.7) is a particular case of (3.8).

3.2 Optimal cross-border trading

The cash process of the agent is denoted by

$$X(t, \mathbf{P}_t, \boldsymbol{\nu}_t) = \boldsymbol{\nu}^\intercal \, \boldsymbol{B}^\intercal \, (\mathbf{P}^{\boldsymbol{\nu}} + \boldsymbol{\Theta}(t)) - \boldsymbol{\nu}^\intercal \, \boldsymbol{\Upsilon} \, \boldsymbol{\nu} \, , \tag{3.9}$$

where

$$\boldsymbol{B} = \begin{pmatrix} -1 & \dots & \dots & -1 & & & & & \\ 1 & & & & -1 & \dots & -1 & & \\ & \ddots & & & 1 & & & & \\ & & \ddots & & & \ddots & & \dots & -1 \\ & & & 1 & & & 1 & & 1 \end{pmatrix}, \qquad \boldsymbol{\Theta}(t) = (\Theta_i(t))_{i=1,\dots,n}\,.$$

The first term on the right-hand side of the process (3.9) represents the cash from trading in the interconnected locations in the absence of trading frictions.

The second term on the right-hand side represents the costs that stem from trading: temporary price impact, interconnector costs, and exchange fees. These costs are represented by $\boldsymbol{\Upsilon}$, with $\boldsymbol{\Upsilon} = \boldsymbol{\Upsilon_1} + \boldsymbol{\Upsilon_2}$. The matrices $\boldsymbol{\Upsilon_1}$ and $\boldsymbol{\Upsilon_2}$ are of dimension $n\,(n-1)/2 \times n\,(n-1)/2$, where $\boldsymbol{\Upsilon_1}$ represents the temporary price impact parameters (i.e., the ω_k parameters in (3.7) and (3.8)), and $\boldsymbol{\Upsilon_2}$ is a diagonal matrix that represents the cost of employing the interconnector and exchange fees.

3.2.1 The value of cross-border trading

The agent's performance criterion and value function are, respectively,

$$Z(t,\mathbf{P};\boldsymbol{\nu}) = \mathbb{E}_{t,\mathbf{P}}\left[\int_t^T X(u,\mathbf{P}_u,\boldsymbol{\nu}_u)\,\mathrm{d}u\right] \qquad \text{and} \qquad V(t,\mathbf{P}) = \sup_{\boldsymbol{\nu}\in\mathcal{A}} Z(t,\mathbf{P};\boldsymbol{\nu})\,. \tag{3.10}$$

The set of admissible strategies, for the constrained case,[8] is

$$\mathcal{A} = \left\{\boldsymbol{\nu} \text{ process with values in } \mathbb{R}^{n\,(n-1)/2} \,:\, \int_0^T \boldsymbol{\nu}_t^\intercal\,\boldsymbol{\nu}_t\,\mathrm{d}t < \infty\,, \quad a.s.\right\}.$$

Here, $\mathbb{E}_{t,\mathbf{P}}[\,\cdot\,]$ denotes the expectation computed when the process $\{\mathbf{P}_u^{\boldsymbol{\nu};t,\mathbf{P}}, u \in [t,T]\}$ is the solution of (3.2) with initial condition $\mathbf{P}_t = \mathbf{P}$ and control $\boldsymbol{\nu}$.

The dynamic programming principle suggests that (3.10) is the unique solution to the

[8] For the unconstrained case the dimensions of the vector $\boldsymbol{\nu}$ and the matrix of permanent price impacts $\boldsymbol{H}$ are as discussed above. All the results that follow from here do not change, only that in the unconstrained case we require each element in $\boldsymbol{\nu}$ to be non-negative.

Hamilton-Jacobi-Bellman (HJB) equation

$$\partial_t V(t,\mathbf{P}) + \sup_{\boldsymbol{\nu}} \left[\mathcal{L}^{\boldsymbol{\nu}} V(t,\mathbf{P}) + X(t,\mathbf{P},\boldsymbol{\nu})\right] = 0\,. \tag{3.11}$$

The infinitesimal generator $\mathcal{L}^{\boldsymbol{\nu}}$ acts on the value function as follows:

$$\begin{aligned}\mathcal{L}^{\boldsymbol{\nu}} V(t,\mathbf{P}) \;&=\; \left(\boldsymbol{\theta} - \boldsymbol{\Phi}\,\mathbf{P} + \boldsymbol{\nu}^\intercal\,\boldsymbol{H}^\intercal\right) V_P(t,\mathbf{P}) + \tfrac{1}{2}\,\mathrm{Tr}\left[\boldsymbol{\Omega}\,\boldsymbol{\mathcal{H}}\right] \\ &\quad + \sum_{k=1}^{n} \lambda_k \int_{-\infty}^{+\infty} \left(\Delta_k(y)\,V\right)(t,\mathbf{P})\,\frac{1}{\sqrt{2\,\pi}\,\xi_k}\,\mathrm{e}^{\frac{-(y-\psi_k)^2}{2\,\xi_k^2}}\,\mathrm{d}y\,,\end{aligned} \tag{3.12}$$

where $V_P(t,\mathbf{P})$ is the vector with elements $\partial V/\partial P_i$, $\mathrm{Tr}[\,\cdot\,]$ denotes the trace operator, $\boldsymbol{\Omega} = \boldsymbol{\sigma}\,\boldsymbol{\sigma}^\intercal$ is the instantaneous variance-covariance matrix of electricity prices, and $\boldsymbol{\mathcal{H}}$ is the Hessian of V; i.e., the matrix with elements $\boldsymbol{\mathcal{H}}_{i,j} = \partial^2 V/\partial P_i\,\partial P_j$. The operator $\Delta_k(y)\,V(t,\mathbf{P})$, due to the jump part of the price process, acts on the value function as follows (see e.g., Cartea et al. (2015) and Øksendal and Sulem (2007)):

$$\Delta_k(y)\,V(t,\mathbf{P}) = V(t,\mathbf{P} + y\,\mathbb{1}_k) - V(t,\mathbf{P})\,, \quad \forall\, k \in \{1,\cdots,n\}\,,$$

where the indicator function $\mathbb{1}_k$ is defined as

$$\mathbb{1}_1 = (1,0,\cdots,0)^\intercal\,, \quad \mathbb{1}_2 = (0,1,\cdots,0)^\intercal\,, \cdots, \quad \mathbb{1}_n = (0,0,\cdots,1)^\intercal\,.$$

Proposition 3.1. *Let the value function* (3.10) *satisfy the HJB* (3.11)*. Then the optimal speed of trading in feedback form is given by*

$$\boldsymbol{\nu}_t^* = \tfrac{1}{2}\,\boldsymbol{\Upsilon}^{-1}\left(\boldsymbol{H}^\intercal\,V_P(t,\boldsymbol{P}) + \boldsymbol{B}^\intercal\,\boldsymbol{P}_t + \boldsymbol{\Theta}(t)\right)\,, \tag{3.13}$$

so that the HJB (3.11) *becomes the partial integro-differential equation (PIDE)*

$$0 = \partial_t V(t,\mathbf{P}) + \mathcal{L}^{\mathbf{0}} V(t,\mathbf{P}) + \tfrac{1}{4}\,\left[\boldsymbol{H}^\intercal\,V_P(t,\boldsymbol{P}) + \boldsymbol{B}^\intercal\,\boldsymbol{P}_t + \boldsymbol{\Theta}(t)\right]^\intercal\,\boldsymbol{\Upsilon}^{-1}\left[\boldsymbol{H}^\intercal\,V_P(t,\boldsymbol{P}) + \boldsymbol{B}^\intercal\,\boldsymbol{P}_t + \boldsymbol{\Theta}(t)\right] \tag{3.14}$$

with $\mathcal{L}^{\mathbf{0}}$ *given by* (3.12) *with* $\boldsymbol{\nu} = \mathbf{0}$*, and recall that* $\boldsymbol{\Upsilon} = \boldsymbol{\Upsilon_1} + \boldsymbol{\Upsilon_2}$*.*

Proof. See Appendix A.2.1. □

We re-write (3.13) as

$$\boldsymbol{\nu}_t^* = \tfrac{1}{2}\,\boldsymbol{\Upsilon}^{-1}\left(\boldsymbol{B}^\intercal\,\boldsymbol{P}_t + \boldsymbol{\Theta}(t)\right) + \tfrac{1}{2}\,\boldsymbol{\Upsilon}^{-1}\boldsymbol{H}^\intercal\,V_P(t,\boldsymbol{P})$$

to explain the intuition of the optimal speed of trading.

The first term on the right-hand side of the equation above represents the optimal speed of trading for an agent who only looks at the spread in prices to decide how to trade (recall that $\boldsymbol{P}$ is the deseasonalised price) and the costs due to temporary price impact, interconnector costs, and exchange fees. This strategy is myopic because it does not incorporate the permanent effect that the agent's trading activity has on the prices of electricity in the various locations. We refer to this strategy as the 'naïve' trading strategy. Note that the naïve strategy does take into account the permanent price impact of the trades of the agent.

The second term on the right-hand side of the equation is the adjustment to the naïve strategy that accounts for the direct and indirect permanent price impacts of the agent's trades on the price of electricity in the various locations, as well as interconnector costs and exchange fees.

Below we employ the naïve strategy as benchmark when we discuss the performance of the optimal cross-border trading strategy and denote it by

$$\boldsymbol{\nu}_t^{\mathrm{n}} = \tfrac{1}{2}\,\boldsymbol{\Upsilon}^{-1}\left(\boldsymbol{B}^\intercal\,\boldsymbol{P}_t + \boldsymbol{\Theta}(t)\right)\,. \tag{3.15}$$

Next, we propose an ansatz to solve the PIDE in (3.14).

Proposition 3.2 (Ansatz)**.** *The PIDE in* (3.14) *admits a solution of the form*

$$V(t,\mathbf{P}) = A(t) + \boldsymbol{D}^\intercal(t)\,\mathbf{P} + \mathbf{P}^\intercal\,\boldsymbol{E}(t)\,\mathbf{P}\,, \tag{3.16}$$

where $A:[0,T]\to\mathbb{R}$, $\boldsymbol{D}:[0,T]\to\mathbb{R}^n$ *and* $\boldsymbol{E}:[0,T]\to\mathbb{R}^{n\times n}$ *are time-dependent functions that solve the Riccati equation*

$$0 = \boldsymbol{E}'(t) + \boldsymbol{E}^\intercal(t)\left(\tfrac{1}{2}\,\boldsymbol{H}\,\boldsymbol{\Upsilon}^{-1}\boldsymbol{B}^\intercal - \boldsymbol{\Phi}\right) + \left(\tfrac{1}{2}\,\boldsymbol{H}\,\boldsymbol{\Upsilon}^{-1}\boldsymbol{B}^\intercal - \boldsymbol{\Phi}\right)^\intercal\boldsymbol{E}(t) + \boldsymbol{E}^\intercal(t)\,\boldsymbol{H}\,\boldsymbol{\Upsilon}^{-1}\,\boldsymbol{H}^\intercal\,\boldsymbol{E}(t) + \tfrac{1}{4}\,\boldsymbol{B}\,\boldsymbol{\Upsilon}^{-1}\,\boldsymbol{B}^\intercal\,; \tag{3.17}$$

the linear equation

$$0 = \boldsymbol{D}'(t) + \left(\tfrac{1}{2}\, \boldsymbol{H}\, \boldsymbol{\Upsilon}^{-1}\, \boldsymbol{B}^{\intercal} - \boldsymbol{\Phi} \right)^{\intercal} \boldsymbol{D}(t) + \boldsymbol{E}^{\intercal}(t)\, \boldsymbol{H}\, \boldsymbol{\Upsilon}^{-1}\, \boldsymbol{H}^{\intercal}\, \boldsymbol{D}(t)$$
$$+ 2\, \boldsymbol{E}(t)(\, \boldsymbol{\theta} + \boldsymbol{\lambda} \circ \boldsymbol{\psi}\,) + \boldsymbol{E}^{\intercal}(t)\, \boldsymbol{H}\, \boldsymbol{\Upsilon}^{-1}\, \boldsymbol{\Theta}(t) + \tfrac{1}{2}\, \boldsymbol{B}\, \boldsymbol{\Upsilon}^{-1}\, \boldsymbol{\Theta}(t)\ ; \tag{3.18}$$

and the integral equation

$$0 = A'(t) + \tfrac{1}{4}\, (\, \boldsymbol{D}^{\intercal}(t)\, \boldsymbol{H} + \boldsymbol{\Theta}^{\intercal}(t)\,)\ \boldsymbol{\Upsilon}^{-1}\ (\, \boldsymbol{H}^{\intercal}\, \boldsymbol{D}(t) + \boldsymbol{\Theta}(t)\,) + \mathrm{Tr}\,[\, \boldsymbol{\Omega}\, \boldsymbol{E}(t)\,]$$
$$+ \boldsymbol{D}^{\intercal}(t)\, (\, \boldsymbol{\theta} + \boldsymbol{\lambda} \circ \boldsymbol{\psi}\,) + \boldsymbol{\psi}^{\intercal}\, diag(\boldsymbol{E}(t))\, (\, \boldsymbol{\lambda} \circ \boldsymbol{\psi}\,) + \boldsymbol{\xi}^{\intercal}\, diag(\boldsymbol{E}(t))\, (\, \boldsymbol{\lambda} \circ \boldsymbol{\xi}\,)\ , \tag{3.19}$$

with terminal condition $A(T) = \boldsymbol{D}(T) = \boldsymbol{E}(T) = 0$.

Here,

$$diag(\boldsymbol{E}(t)) = \begin{pmatrix} E_{11}(t) & 0 & 0 \\ 0 & \ddots & 0 \\ 0 & 0 & E_{nn}(t) \end{pmatrix},$$

where the entries $E_{11}(t), \ldots, E_{nn}(t)$ *are the diagonal elements of the matrix* $\boldsymbol{E}(t)$*, and the operator* $\circ$ *denotes the Hadamard product between two vectors, i.e.,* $\boldsymbol{\lambda} \circ \boldsymbol{\psi} = (\lambda_1\, \psi_1, \ldots, \lambda_n\, \psi_n)$.

Thus, the candidate optimal control in (3.13) *is*

$$\boldsymbol{\nu}_t^* = \boldsymbol{\Upsilon}^{-1} \left(\tfrac{1}{2}\, \boldsymbol{H}^{\intercal}\, \boldsymbol{D}(t) + \boldsymbol{H}^{\intercal}\, \boldsymbol{E}(t)\, \boldsymbol{P}_t + \tfrac{1}{2}\, \boldsymbol{B}^{\intercal}\, \boldsymbol{P}_t + \tfrac{1}{2}\, \boldsymbol{\Theta}(t) \right)\ . \tag{3.20}$$

Proof. See Appendix A.2.2. □

3.3 Implementation of cross-border strategy

As stated in Proposition 3.2, the HJB equation admits an explicit solution up to the system of three equations: (3.17), (3.18), (3.19). We use the representation $\boldsymbol{E}(t) = \boldsymbol{Y}(t)\, \boldsymbol{X}(t)^{-1}$ in Gombani and Runggaldier (2013) to solve the Riccati equation in (3.17), where $\boldsymbol{X}$ and $\boldsymbol{Y}$ satisfy the linear differential equation

$$\frac{\partial}{\partial t} \begin{pmatrix} \boldsymbol{X} \\ \boldsymbol{Y} \end{pmatrix} = \boldsymbol{M} \begin{pmatrix} \boldsymbol{X} \\ \boldsymbol{Y} \end{pmatrix} \qquad \text{with final condition} \qquad \begin{pmatrix} \boldsymbol{X}(T) \\ \boldsymbol{Y}(T) \end{pmatrix} = \begin{pmatrix} \boldsymbol{I} \\ 0 \end{pmatrix}, \tag{3.21}$$

where

$$\boldsymbol{M} = \begin{pmatrix} \frac{1}{2}\,\boldsymbol{H}\,\boldsymbol{\Upsilon}^{-1}\,\boldsymbol{B}^{\intercal} - \boldsymbol{\Phi} & \boldsymbol{H}\,\boldsymbol{\Upsilon}^{-1}\,\boldsymbol{H}^{\intercal} \\ -\frac{1}{4}\,\boldsymbol{B}\,\boldsymbol{\Upsilon}^{-1}\,\boldsymbol{B}^{\intercal} & -\frac{1}{2}\,\left(\boldsymbol{H}\,\boldsymbol{\Upsilon}^{-1}\,\boldsymbol{B}^{\intercal} - \boldsymbol{\Phi}\right)^{\intercal} \end{pmatrix}.$$

It is straightforward to show that the solution to (3.21) is

$$\begin{pmatrix} \boldsymbol{X}(t) \\ \boldsymbol{Y}(t) \end{pmatrix} = \exp\left[-(T-t)\,\boldsymbol{M}\right] \begin{pmatrix} \boldsymbol{X}(T) \\ \boldsymbol{Y}(T) \end{pmatrix}. \tag{3.22}$$

The numerical implementation of (3.22) is unstable for high values of the terminal date T. The spectrum of $\boldsymbol{M}$ is symmetric with respect to the imaginary axis and has no purely imaginary eigenvalues, see Bini et al. (2012). Thus, the eigenvalues of $\boldsymbol{M}$ come in pairs with same imaginary parts, and real parts with same absolute values and of opposite sign. Hence, as time evolves, the solution in (3.22) explodes due to the eigenvalues with positive real part, which causes numerical instabilities when one computes $\boldsymbol{X}^{-1}$.

Here, we use the solution representation of Vaughan (1969) to circumvent numerical instabilities. Specifically, we write

$$\boldsymbol{M} = \boldsymbol{W} \begin{pmatrix} \boldsymbol{\Lambda} & 0 \\ 0 & -\boldsymbol{\Lambda} \end{pmatrix} \boldsymbol{W}^{-1}, \tag{3.23}$$

where $\boldsymbol{\Lambda}$ is a diagonal matrix where the real parts of its n eigenvalues are positive (and thus cause numerical instabilities), and

$$\boldsymbol{W} = \begin{pmatrix} \boldsymbol{W}_{11} & \boldsymbol{W}_{12} \\ \boldsymbol{W}_{21} & \boldsymbol{W}_{22} \end{pmatrix} \tag{3.24}$$

is the matrix of eigenvectors, where each $\boldsymbol{W}_{ij}$ is a $n \times n$ matrix. Define

$$\boldsymbol{R} = -\left[\boldsymbol{W}_{22} - \boldsymbol{E}(T)\,\boldsymbol{W}_{12}\right]^{-1}\left[\boldsymbol{W}_{21} - \boldsymbol{E}(T)\,\boldsymbol{W}_{11}\right] = -\boldsymbol{W}_{22}^{-1}\,\boldsymbol{W}_{21}, \tag{3.25}$$

and

$$\boldsymbol{G}(t) = e^{-\boldsymbol{\Lambda}\,(T-t)}\,\boldsymbol{R}\,e^{-\boldsymbol{\Lambda}\,(T-t)}. \tag{3.26}$$

Then,

$$\boldsymbol{E}(t) = \boldsymbol{N}(t)\,\boldsymbol{Q}(t)^{-1}, \qquad \text{where} \begin{cases} \boldsymbol{N}(t) &= \boldsymbol{W}_{21} + \boldsymbol{W}_{22}\,\boldsymbol{G}(t), \\ \boldsymbol{Q}(t) &= \boldsymbol{W}_{11} + \boldsymbol{W}_{12}\,\boldsymbol{G}(t). \end{cases} \tag{3.27}$$

This formulation provides a numerically stable solution of $\boldsymbol{E}(t)$ because the only time-varying terms are the negative exponentials in (3.26).

The solution to (3.18) is

$$\boldsymbol{D}(t) = \int_t^T \exp\left\{ \int_s^T \left[\left(\tfrac{1}{2}\, \boldsymbol{H}\, \boldsymbol{\Upsilon}^{-1}\, \boldsymbol{B}^\intercal - \boldsymbol{\Phi} \right)^\intercal + \boldsymbol{E}^\intercal(u)\, \boldsymbol{H}\, \boldsymbol{\Upsilon}^{-1}\, \boldsymbol{H}^\intercal \right] \mathrm{d}u \right\}$$
$$\times \left\{ 2\, \boldsymbol{E}(s)\, (\boldsymbol{\theta} + \boldsymbol{\lambda} \circ \boldsymbol{\psi}) + \boldsymbol{E}^\intercal(s)\, \boldsymbol{H}\, \boldsymbol{\Upsilon}^{-1}\, \boldsymbol{\Theta}(s) + \tfrac{1}{2}\, \boldsymbol{B}\, \boldsymbol{\Upsilon}^{-1}\, \boldsymbol{\Theta}(s) \right\} \mathrm{d}s\,. \tag{3.28}$$

Finally,

$$A(t) = A(T) + \int_t^T \tfrac{1}{4}\, \left(\boldsymbol{D}^\intercal(s)\, \boldsymbol{H} + \boldsymbol{\Theta}^\intercal(s) \right) \boldsymbol{\Upsilon}^{-1}\, \left(\boldsymbol{H}^\intercal\, \boldsymbol{D}(s) + \boldsymbol{\Theta}(s) \right) + \mathrm{Tr}\left[\boldsymbol{\Omega}\, \boldsymbol{E}(s) \right]$$
$$+ \boldsymbol{D}^\intercal(s)\, \left(\boldsymbol{\theta} + \boldsymbol{\lambda} \circ \boldsymbol{\psi} \right) + \boldsymbol{\psi}^\intercal\, diag(\boldsymbol{E}(s))\, \left(\boldsymbol{\lambda} \circ \boldsymbol{\psi} \right) + \boldsymbol{\xi}^\intercal\, diag(\boldsymbol{E}(s))\, \left(\boldsymbol{\lambda} \circ \boldsymbol{\xi} \right) \mathrm{d}s\,, \tag{3.29}$$

where one can evaluate the integrals in (3.28) and (3.29) with a quadrature method or with a recursive scheme.

4 Estimation of model parameters

Here, we estimate the parameters of model (3.2), so that in the next section we evaluate the financial performance of the cross-border trading strategy. In particular, in this section we provide empirical support to the main novelty of model (3.2), i.e., the permanent price impact function $g(\boldsymbol{\nu_t})$ that captures the effect of electricity flows on prices in all locations of the network.

We focus on a model with $n = 3$ locations to trade power in France, Germany, and Switzerland. First, we estimate the impact that electricity flows between locations has on the price of electricity in the three countries. That is, we estimate the parameters of the matrix $\boldsymbol{H}$ in (3.5). The permanent price impact parameters in $\boldsymbol{H}$ are denoted by $\beta_{\cdot\cdot}$. Let

$$\boldsymbol{P}_t = \begin{pmatrix} P_t^F & P_t^S & P_t^G \end{pmatrix}^\intercal, \qquad \Delta \boldsymbol{P}_t = \boldsymbol{P}_t - \boldsymbol{P}_{t-1}\,,$$

where $^\intercal$ denotes the transpose operator, and the entries in the price vector $\boldsymbol{P}_t$ are denoted by P_t^i, where $i = F, G, S$ represents the location France, Germany, Switzerland, respectively. Moreover, let v_t^{ij} be the volumes of the transactions, where $i, j \in \{F, G, S, O\}$ and O denotes other countries (Austria, Belgium, Luxembourg, and the Netherlands). For example, the variable v_{t-1}^{SF} represents the quantity of power bought in Switzerland and sold in France, traded

at time $t-1$ (exports and imports for the other locations are denoted in a similar way). As mentioned in Section 3, the cross-border impact that the speeds of trading ν_{ij} and ν_{ji} have on the prices: i) may be different (unconstrained), or ii) are symmetric (constrained). Thus, we run two regressions:

i) Unconstrained:

$$\begin{aligned}\Delta \boldsymbol{P}_t &= \boldsymbol{\beta}_{SF}\,\mathrm{v}^{SF}_{t-1} + \boldsymbol{\beta}_{FS}\,\mathrm{v}^{FS}_{t-1} + \boldsymbol{\beta}_{GS}\,\mathrm{v}^{GS}_{t-1} + \boldsymbol{\beta}_{SG}\,\mathrm{v}^{SG}_{t-1} + \boldsymbol{\beta}_{GF}\,\mathrm{v}^{GF}_{t-1} + \boldsymbol{\beta}_{FG}\,\mathrm{v}^{FG}_{t-1} \\ &\quad + \boldsymbol{\beta}_{OF}\,\mathrm{v}^{OF}_{t-1} + \boldsymbol{\beta}_{FO}\,\mathrm{v}^{FO}_{t-1} + \boldsymbol{\beta}_{OS}\,\mathrm{v}^{OS}_{t-1} + \boldsymbol{\beta}_{SO}\,\mathrm{v}^{SO}_{t-1} \\ &\quad + \boldsymbol{\beta}_{OG}\,\mathrm{v}^{OG}_{t-1} + \boldsymbol{\beta}_{GO}\,\mathrm{v}^{GO}_{t-1} + \boldsymbol{\varepsilon}_t\,;\end{aligned} \tag{4.1}$$

ii) Constrained:

$$\begin{aligned}\Delta \boldsymbol{P}_t &= \boldsymbol{\beta}_1\,\left(\mathrm{v}^{SF}_{t-1} - \mathrm{v}^{FS}_{t-1}\right) + \boldsymbol{\beta}_2\,\left(\mathrm{v}^{GS}_{t-1} - \mathrm{v}^{SG}_{t-1}\right) + \boldsymbol{\beta}_3\,\left(\mathrm{v}^{GF}_{t-1} - \mathrm{v}^{FG}_{t-1}\right) \\ &\quad + \boldsymbol{\beta}_4\,\left(\mathrm{v}^{FO}_{t-1} - \mathrm{v}^{OF}_{t-1}\right) + \boldsymbol{\beta}_5\,\left(\mathrm{v}^{SO}_{t-1} - \mathrm{v}^{OS}_{t-1}\right) + \boldsymbol{\beta}_6\,\left(\mathrm{v}^{GO}_{t-1} - \mathrm{v}^{OG}_{t-1}\right) + \boldsymbol{\varepsilon}_t\,,\end{aligned} \tag{4.2}$$

where $\boldsymbol{\varepsilon}_t$ is a three-dimensional vector of i.i.d. normally distributed error terms. Equations (4.1) and (4.2) are discretised versions of (3.2), where we disregard the co-integration effects. We run the multivariate ordinary least squares (OLS) regressions with a stepwise algorithm.

We consider power delivered at different hours of the day as different products; thus, we pool data by hour of delivery and run 24 independent regressions, one for each hour of the day, as specified in (4.1) or (4.2). Furthermore, we only take into account the last 10 hours of trading for each contract before the start of delivery because the rate of trading activity typically increases as the delivery time of power approaches. We assume that the increments of t are in intervals of 5 minutes to ensure that there are transactions over that time window. If there are multiple transactions for a single variable over a 5-minute interval, we consider the price observation P^i_t of the first transaction that occurred in that interval for country i, and compute the quantity V^{ij}_t as the sum of the ij quantities of all transactions occurred during the same interval in the ij trade direction. Moreover, price observations that deviate more than three standard deviations from the mean price of the hourly contract are considered outliers,

so we discard them.[9]

In the unconstrained regression (4.1), the parameters for direct and indirect permanent price impact are denoted by $\boldsymbol{\beta}_{SF}, \ldots, \boldsymbol{\beta}_{GO}$. And in the constrained regression (4.2), the parameters are denoted by $\boldsymbol{\beta}_1, \ldots, \boldsymbol{\beta}_6$. Note that $\boldsymbol{\beta}_{SF}, \ldots, \boldsymbol{\beta}_{FG}$ and $\boldsymbol{\beta}_1, \ldots, \boldsymbol{\beta}_3$ represent the permanent price impact parameters (direct and indirect) for the imports and exports in the three countries we study. And the parameters $\boldsymbol{\beta}_{OF}, \ldots, \boldsymbol{\beta}_{GO}$ and $\boldsymbol{\beta}_4, \ldots, \boldsymbol{\beta}_6$ represent the permanent price impact (direct and indirect) that the other countries of the power network have on the prices of France, Germany, and Switzerland.

As mentioned, we employ a stepwise regression (see Draper and Smith, 1998) to select the relevant regressors in models (4.1) and (4.2). The algorithm adds or removes regressors based on their statistical significance, and compares the explanatory power of incrementally larger and smaller models. In the first iteration of the algorithm, we set the parameters $\boldsymbol{\beta}_{OF}, \ldots, \boldsymbol{\beta}_{GO}$ and $\boldsymbol{\beta}_3, \ldots, \boldsymbol{\beta}_6$ to zero. In the subsequent iterations, the algorithm includes and excludes parameters depending on a tolerance level of the p-value of the parameter – we set this level at 0.10.

Table 6 shows the coefficient estimates of the stepwise regression for the contract that delivers on the hour ending at 2pm (i.e., contracts for power delivered between 1pm and 2pm) for the unconstrained case (4.1). The coefficient estimates of the constrained regression (4.2) for all other hourly products are reported in Appendix A.1, Tables 13–15. The tables with the coefficient estimates of the unconstrained model (4.1) for all other hourly products are not reported in the paper for brevity and are available upon request. The results show that there are significant direct permanent price impacts in the price dynamics, i.e., buying (selling) electricity in one location exerts an upward (downward) pressure on the price of electricity in that location.

For example, in the German market, the values of the parameter estimates $\hat{\beta}_{SF}, \cdots, \hat{\beta}_{GO}$ in the third column of Table 6 provide the marginal change in the dependent variable ΔP_t^G when there is a change in one of the explanatory variables on the right-hand side (holding all other explanatory variables fixed). The values of the parameters $\hat{\beta}_{GS}$, $\hat{\beta}_{SG}$, $\hat{\beta}_{GF}$, $\hat{\beta}_{OG}$, $\hat{\beta}_{GO}$ show that an increase in the power supply (increase in the demand of power) in Germany, exerts a downward (upward) pressure on the price of power in Germany. The estimates $\hat{\beta}_{SF}$, $\hat{\beta}_{FS}$ in the first column and $\hat{\beta}_{SF}$, $\hat{\beta}_{FS}$, $\hat{\beta}_{OS}$ in the second column, represent the direct permanent effects

[9] On average, we discard 1.12%, 1.51%, and 0.48% of the transactions for France, Germany, and Switzerland, respectively, for each hourly contract.

that the volumes, exported from or imported into France and Switzerland, have on the prices of France and Switzerland, respectively. The estimate $\hat{\beta}_{SF}$ in Table 6 shows that when the agent buys electricity in Switzerland to export it to France, she exerts an upward pressure on the price of power in Switzerland and a downward pressure on the price of power in France.

Our results show that for most hours, the direct permanent price impact is statistically significant for each country: positive when exporting and negative when importing. The few exceptions are for off-peak contracts for electricity in Switzerland, which is the country with the least number of internal transactions (smaller sample compared with France and Germany).

The results in Table 6 (and in Tables 13–15) also show that trading activity between two interconnected locations can have an indirect permanent price impact on the price of electricity in another location that is part of the interconnected electricity network. For example, the parameter $\hat{\beta}_{FS}$ in the third column of Table 6 is negative and statistically significant, that is, contracts for power exported from France into Switzerland have a downward pressure on the price of electricity in Germany.

	ΔP_t^F	ΔP_t^S	ΔP_t^G
Unconstrained (4.1)			
$\hat{\boldsymbol{\beta}}_{SF}$	-0.0013^{***}	0.0031^{***}	0
$\hat{\boldsymbol{\beta}}_{FS}$	0.0024^{***}	-0.0007^{***}	-0.0012^{**}
$\hat{\boldsymbol{\beta}}_{GS}$	0.0007^{***}	0	0.0025^{***}
$\hat{\boldsymbol{\beta}}_{SG}$	0	0	-0.0045^{***}
$\hat{\boldsymbol{\beta}}_{GF}$	0	0	0.0011^{*}
$\hat{\boldsymbol{\beta}}_{FG}$	0	0	0
$\hat{\boldsymbol{\beta}}_{OF}$	0	-0.0010^{*}	0
$\hat{\boldsymbol{\beta}}_{FO}$	0	0	0
$\hat{\boldsymbol{\beta}}_{OS}$	0	-0.0028^{**}	0
$\hat{\boldsymbol{\beta}}_{SO}$	0.0020^{**}	0	0
$\hat{\boldsymbol{\beta}}_{OG}$	0	-0.0012^{**}	-0.0019^{*}
$\hat{\boldsymbol{\beta}}_{GO}$	0	0	0.0028^{***}
Constrained (4.2)			
$\hat{\boldsymbol{\beta}}_{1}$	-0.0021^{***}	0.0015^{***}	0
$\hat{\boldsymbol{\beta}}_{2}$	0	0.0016^{*}	0
$\hat{\boldsymbol{\beta}}_{3}$	0	0	-0.0010^{*}

Table 6: OLS robust estimates, with stepwise algorithm, for unconstrained (4.1) and constrained (4.2) specifications for contracts with delivery on the hour ending at 2pm. Dependent variables: ΔP_t^F, ΔP_t^S, ΔP_t^G. Notation: $^{***} = p < 0.01, ^{**} = p < 0.05, ^{*} = p < 0.1$.

4.1 Seasonality and other model parameters

Table 7 reports the seasonality parameters in (3.1), estimated with OLS. The estimates of the other model parameters in (3.2) are obtained by Maximum Likelihood Estimation (MLE). We

	b_1	b_2	b_3	b_4	b_5	b_6
P^F	-5.79	16.47	-4.70	5.43	9.02	38.96
	(-4.67)	(13.32)	(-3.91)	(4.63)	(5.15)	(22.27)
P^S	-5.02	22.43	-1.15	7.84	11.91	37.54
	(-2.10)	(9.42)	(-0.50)	(3.47)	(3.53)	(11.15)
P^G	-3.45	11.65	-0.86	4.79	8.92	29.02
	(-2.93)	(9.92)	(-0.76)	(4.30)	(5.36)	(17.48)

Table 7: OLS parameter estimates of model (3.1) for electricity delivered at 11am, t-stats in parenthesis.

use closing prices from our transaction data – with a slight abuse of notation, we assume that the unit of t is one day. The discretised version of (3.2) is

$$\boldsymbol{P}_{t+1} = \boldsymbol{\theta} + (\boldsymbol{I} - \boldsymbol{\Phi})\,\boldsymbol{P}_t + \boldsymbol{H}\,\boldsymbol{\nu}_t + \boldsymbol{\sigma}\,\varepsilon_t + (\boldsymbol{\psi} + \boldsymbol{\xi}\,\varepsilon_{Jt})\,\boldsymbol{Y}_\lambda\,, \tag{4.3}$$

where $\boldsymbol{I}$ is the identity matrix, $(\varepsilon_t)_t$ and $(\varepsilon_{Jt})_t$ are i.i.d. sequences of standard normal random variables, also independent of each other, and

$$\boldsymbol{Y}_\lambda = \begin{pmatrix} Y_1^{\lambda_1} & 0 & \cdots & 0 \\ 0 & Y_2^{\lambda_2} & \ddots & \vdots \\ \vdots & \ddots & \ddots & 0 \\ 0 & \cdots & 0 & Y_n^{\lambda_n} \end{pmatrix},$$

with $Y_k^{\lambda_k} \sim \text{Bern}(\lambda_k)$ independent of $Y_i^{\lambda_i}$, $\forall\, k \neq i$, $k = 1, \cdots, n$. In the absence of the agent's cross-border trades (i.e., $\boldsymbol{\nu} = \boldsymbol{0}$), we estimate the remaining parameters of the model. To this end, write the multivariate conditional density function as

$$\begin{aligned} f\,(\boldsymbol{P}_{t+1} \mid \boldsymbol{P}_t) \;=\; & \sum_{\mathrm{e}\,\in E} \left[\prod_{i=1}^{n} \lambda_i^{\mathrm{e}_i} \left(1 - \lambda_i^{1-\mathrm{e}_i}\right)\right] (2\,\pi)^{-n/2} \det\left(\,\boldsymbol{\Omega} + \boldsymbol{\xi}_{\mathrm{e}}\,\right)^{-1/2} \\ & \times \exp\Big\{ -\tfrac{1}{2}\,[\boldsymbol{P}_{t+1} - \boldsymbol{\psi}_{\mathrm{e}} + \boldsymbol{\theta} + (\boldsymbol{I} - \boldsymbol{\Phi})\,\boldsymbol{P}_t]^{\intercal} \\ & \times (\boldsymbol{\Omega} + \boldsymbol{\xi}_{\mathrm{e}})^{-1}\,[\boldsymbol{P}_{t+1} - \boldsymbol{\psi}_{\mathrm{e}} + \boldsymbol{\theta} + (\boldsymbol{I} - \boldsymbol{\Phi})\,\boldsymbol{P}_t] \Big\}\,, \end{aligned} \tag{4.4}$$

where $\boldsymbol{\Omega} = \boldsymbol{\sigma}\,\boldsymbol{\sigma}^{\intercal}$, and $\det(\,\cdot\,)$ represents the determinant of a matrix. Let $E = \{0,1\}^n$, then, $\forall\, \mathrm{e} \in E$, $\boldsymbol{\xi}_{\mathrm{e}}$ is the $n \times n$ diagonal matrix with elements $(\xi_{\mathrm{e}})_{ii} = \xi_{ii}^2\,\mathrm{e}_i$ and $(\xi_{\mathrm{e}})_{ij} = 0\,,\ \forall\, i \neq j$. Similarly, $\boldsymbol{\psi}_{\mathrm{e}}$ is a vector with n elements $(\psi_{\mathrm{e}})_i = \psi_i\,\mathrm{e}_i$.

Table 8 reports the estimates that result from a numerical maximisation of the log-likelihood function for $n = 3$. Figure 1 shows simulated in-sample and out-of-sample paths of the non-deseasonalised price process $(\widetilde{P}_t^k)_{t>0}$, for a peak hour (11am).

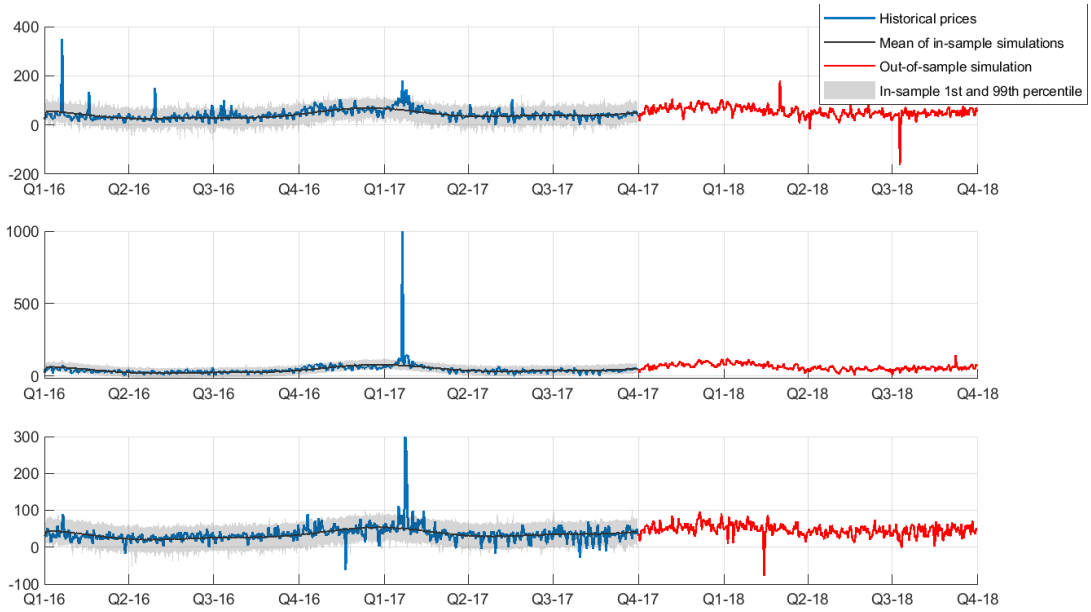

Figure 1: Historical and simulated non-deseasonalised electricity price paths for contracts with peak delivery at 11am, for France (top panel), Switzerland (middle panel) and Germany (bottom panel). The blue solid line represents the historical price path, and the red line represents a single out-of-sample price simulation. The grey area represents the 1^{st} and 99^{th} percentiles of all in-sample simulations, and the black solid line is their mean. Prices are in €/MW.

		France	Switzerland	Germany
Φ	France	0.77 (15.97)	−0.06 (−3.45)	−0.12 (−5.12)
	Switzerland	−0.06 (−3.45)	0.63 (18.55)	−0.03 (−2.05)
	Germany	−0.12 (−5.12)	−0.03 (−2.05)	0.91 (17.92)
σ	France	11.79 (6.14)	0 (-)	0 (-)
	Switzerland	6.70 (14.73)	8.00 (4.54)	0 (-)
	Germany	6.94 (12.12)	1.77 (0.98)	9.80 (6.08)
θ		−1.51 (−1.37)	−1.10 (−1.41)	−0.47 (−0.67)
ψ		0.06 (0.34)	−4.24 (−22.84)	−9.44 (−50.83)
diag(ξ)		70.17 (162.81)	48.08 (111.56)	72.31 (167.77)
λ		0.03 (0.43)	0.04 (0.45)	0.02 (0.34)

Table 8: Parameter estimates of (3.2) obtained with MLE using daily closing prices of intraday hourly contracts with delivery at 11am. The t-stats are reported in parentheses.

Table 8 also reports the estimates of the elements of the matrix $\mathbf{\Phi}$, which show that the evolution of the price of electricity in France depends on past values of prices in Switzerland (0.14) more than it does on those of Germany (0.06). And the price in Switzerland depends more on past values of prices in France than on the prices in Germany. Moreover, the estimated coefficients of the elements of $\boldsymbol{\sigma}$ show that the prices in France and Switzerland also have a high degree of correlation (0.64), greater than that between France and Germany (0.57) and that between Germany and Switzerland (0.48).

There are many models that are designed to capture the stylised facts of price dynamics. However, we remark that our choice is key in the setup of the agent's stochastic control problem because we obtain the optimal cross-border strategy in closed-form – other models may lead to trading strategies that must be solved numerically.

5 Performance of trading strategy

In this section we illustrate the performance of the cross-border trading strategy for one year of trading ($T = 365$ days). We employ the closed-form solution derived in Proposition 3.2. Recall that the closed-form solution we find is for the constrained case, that is, when the permanent price impact of trades between two locations is symmetric.

Here, we assume that the agent trades in three interconnected locations: France, Germany, Switzerland, and that the execution prices received by the agent are as in (3.7). The speed of trading is the vector

$$\boldsymbol{\nu}_t = \begin{pmatrix} \nu_t^{SF} & \nu_t^{GS} & \nu_t^{GF} \end{pmatrix}^\intercal$$

and we employ the discretised version of the price process (3.2) to simulate 1,000 price paths with a time step of 1/50 day – the results discussed here do not change for smaller time steps. To streamline the discussion, we focus on the performance of the strategy for the 11am contract, after which we discuss the results of the strategy for the remaining hours of the day.

For each price path, the agent employs the results in Proposition 3.2 to compute the quantity of electricity to trade in the various locations and we keep track of the accumulated cash $X_t^{\nu^*}$ for the optimal strategy and the accumulated cash $X_t^{\nu^{\mathrm{n}}}$ for the naïve strategy that trades at the speed in (3.15). As benchmark of performance, we compare the profit obtained by the optimal trading strategy with the profits obtained from the naïve strategy.

For the price simulations and cross-border price impact, we employ the parameters in Tables

7, 8, 13, 14, 15, and assume that the country-specific temporary price impact parameters are $\omega_k = 0.01$ €/MW^2 for all countries, see Glas et al. (2019) for a study of the temporary price impact of orders in the EPEX exchange. Therefore the value of the diagonal entries in $\boldsymbol{\Upsilon_1}$ is 0.02 – each transaction incurs temporary price impact in the buy location and in the sell location. In the first instance, we also assume that there are no exchange fees and we assume that interconnector costs are zero (i.e., $\boldsymbol{\Upsilon_2} = \mathbf{0}$), thus, these results over-estimate the profits of the strategy. Below, in Subsection 5.1 we discuss the performance of the strategy for a range of interconnector costs and exchange fees, where we observe that profits drop as costs increase.

The left panel of Figure 2 shows the mean of the trading speeds when the agent employs the optimal strategy (3.20) for the 11am hour. Recall that we do not impose a constraint on the trading speed, which should be capped by the $\text{atc}_t \leq \text{ATC}$, that is by the remaining available transfer capacity at time t. For these simulations, the percentage of days where the speed of trading exceeds the ATC for hour 11am is 0.57% (Switzerland to France), 0.13% (France to Switzerland), 48.74% (Germany to Switzerland), 0.08% (Switzerland to Germany), 0.59% (Germany to France), and 0.23% (France to Germany). The right-hand panel of the figure shows the difference between the average speeds of the optimal and the naïve strategies. Recall that the naïve speed does not account for the permanent impact that the imports and exports of electricity have on prices, we return to this point at the end of this subsection.

Figure 3 shows the cash process for the 11am hourly contract. As expected, the optimal strategy outperforms the naïve strategy. The dash-blue (dash-red) line depicts the cash process of the optimal (naïve) strategy. The height of the blue area shows the difference between the cumulative cash obtained from the optimal and the naïve strategies. The bottom figures show the cumulative cash obtained from each of the three bilateral transmission lines. At the end of the trading horizon T, the optimal strategy obtains on average €5,803,100, with a 95% confidence interval of $[5,786,900; 5,819,300]$. The naïve strategy obtains €5,253,700, with a 95% confidence interval of $[5,238,700; 5,268,800]$.

For the 24 hours, the outperformance of the optimal strategy over the naïve strategy ranges between around €0 (hour 6am) and €6,409,700 (hour 10am) at the end of one year of trading. Compared with the naïve strategy, the optimal strategy performs best in contracts with delivery on the hours that end at 10am, 3am, and 8am. In particular, the average profits of the optimal strategy are approximately 60%, 38%, and 13% (respectively) higher than those obtained with the naïve strategy. On the other hand, the outperformance of the optimal strategy is lowest for

the hours with deliveries that end at 6am, 10pm, and 12am – the average profits are 0%, 0.06%, and 0.10% (respectively) higher than those obtained with the naïve strategy. On average, for the 24 hours, the optimal strategy earns about 6.05% more than the naïve strategy.

The average profit obtained with the optimal cross-border strategy when trading the 24 hourly contracts is €130,209,000, with a 95% confidence interval of [130, 110, 800; 130, 307, 100], and the agent trades on average 293,922,000 MW. Thus, the strategy's average profits are 0.44€/MWh – the naïve strategy's average profits are 0.50€/MWh (i.e., €118,771,200, in [118, 682, 300; 118, 860, 100], for a total of 238,332,000 MW). Similarly, Table 9 reports the €/MWh profits for each hour. Observe that the profits per hour are higher for peak contracts.

Finally, Table 10 reports the mean cross-border volume per transaction, for each trading direction. We see that Germany is the country with the highest exports, followed by France, and Switzerland is the country with the highest imports.

01:00	02:00	03:00	04:00	05:00	06:00	07:00	08:00
0.43	0.37	0.25	0.38	0.44	0.44	0.48	0.38
09:00	10:00	11:00	12:00	13:00	14:00	15:00	16:00
0.60	0.51	0.32	0.42	0.48	0.48	0.48	0.55
17:00	18:00	19:00	20:00	21:00	22:00	23:00	24:00
0.46	0.57	0.86	0.51	0.41	0.35	0.34	0.34

Table 9: Gross optimal strategy profits, expressed in €/MWh, for each hourly contract.

CH-FR	FR-CH	DE-CH	CH-DE	DE-FR	FR-DE
40.72	109.21	410.42	59.33	293.44	77.92

Table 10: Mean volume per transaction (in MW) traded with the optimal trading strategy.

Recall that to obtain a closed-form solution to the stochastic control problem we did not constrain the strategies by the ATC levels reported in Table 2. Thus, to understand the impact of the ATC constraint, we adopt a conservative approach and compute the profits of a "capped strategy" in which the cumulative optimal controls $\boldsymbol{\nu}_t^*$ over each trading day are capped at the corresponding ATC. The discretized version of the capped speed of trading for the border ij

that we use for implementation is

$$\nu_t^{ij} = \begin{cases} \nu^{ij*}_t & \text{if} \quad \left\{0 \le \sum_{s=t_s}^{t\le t_e} \nu^{ij*}_s \le ATC^{ij}\right\} \text{ or } \left\{-ATC^{ji} \le \sum_{s=t_s}^{t\le t_e} \nu^{ij*}_s \le 0\right\}, \\ ATC^{ij} - \sum_{s=t_s}^{(t-1)\le t_e} \nu^{ij*}_s & \text{if} \quad \sum_{s=t_s}^{t\le t_e} \nu^{ij*}_s \ge ATC^{ij}, \\ -ATC^{ji} - \sum_{s=t_s}^{(t-1)\le t_e} \nu^{ij*}_s & \text{if} \quad \sum_{s=t_s}^{t\le t_e} \nu^{ij*}_s \le -ATC^{ji}, \end{cases} \tag{5.1}$$

where t_s and t_e represent the beginning and the end of the trading day, respectively. In the constrained trading speed in (5.1), we see that over each trading day the controls in opposite trading directions offset each other, so that, throughout the trading day, the ATC only limits the net position from one country to another. Table 11 reports the €/MWh profits of such a strategy for each hour. When trading all 24 hourly contracts, the average profits are 0.31€/MWh (€9,921,600 for a total of 32,345,000 MW). The profits of the capped strategy are a conservative lower bound of the profits that could be obtained if the ATC constraint was explicitly accounted for in the computation of the optimal speed of trading.

01:00	02:00	03:00	04:00	05:00	06:00	07:00	08:00
0.31	0.28	0.16	0.27	0.29	0.28	0.36	0.27
09:00	10:00	11:00	12:00	13:00	14:00	15:00	16:00
0.43	0.26	0.27	0.30	0.31	0.32	0.31	0.34
17:00	18:00	19:00	20:00	21:00	22:00	23:00	24:00
0.31	0.38	0.58	0.34	0.26	0.26	0.27	0.26

Table 11: Gross strategy profits, expressed in €/MWh, for each hourly contract, where the cumulative optimal controls $\boldsymbol{\nu}_t^*$ over each trading day are capped at the ATC levels reported in Table 2.

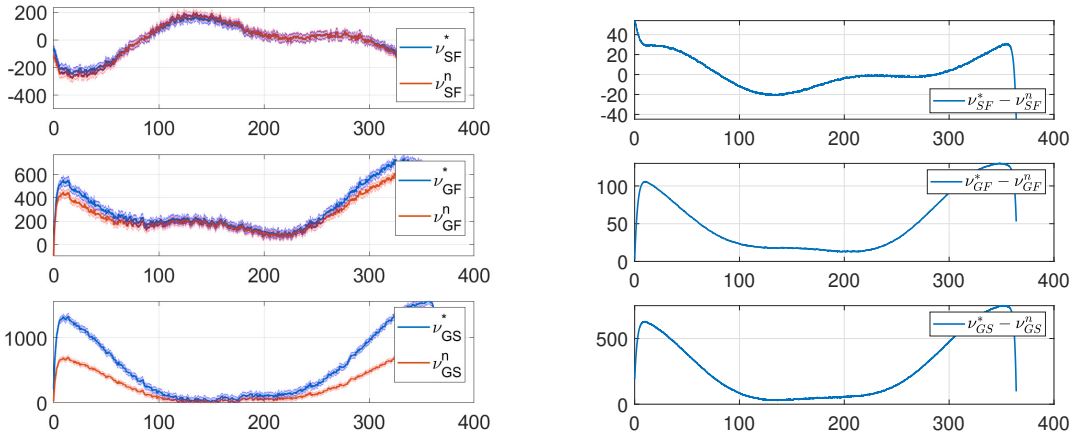

Figure 2: Optimal and naïve speeds, ν^* and ν^n respectively, with their 99% confidence bands (left panel) and difference between them (right panel), for 11am. Trading horizon $T = 365$ days.

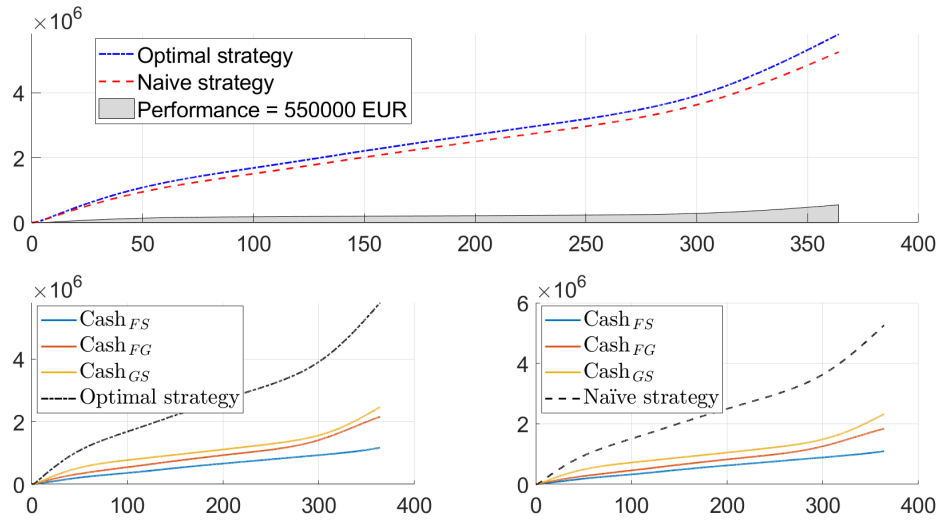

Figure 3: Cumulative cash for 11am contracts. The blue-dash line in the upper panel represents the cumulative cash flows from optimal trading strategy, while the red-dash line, upper panel, is from the naïve trading strategy. The solid yellow, red and blue lines depict the revenue from trading in contracts between Germany-Switzerland, Germany-France and France-Switzerland, respectively, with the optimal (left bottom panel) and the naïve strategies (right bottom panel).

5.1 Interconnector costs and exchange fees

K	1	2	3	4	5	10	15	20
Profit (10^6 €)	130	57	37	28	22	11	7	5
Volume (10^6 MWh)	295	120	77	57	45	22	15	11
Profit/MWh	0.443	0.472	0.482	0.485	0.487	0.490	0.491	0.492
Cost/MWh	0.287	0.168	0.153	0.148	0.146	0.142	0.141	0.141
ATC breaches in %								
FR-CH	0.267	0.014	0.001	0	0	0	0	0
CH-FR	0.055	0.001	0	0	0	0	0	0
DE-CH	23.749	2.810	0.684	0.260	0.102	0.001	0	0
CH-DE	0.101	0.001	0	0	0	0	0	0
DE-FR	0.441	0.016	0	0	0	0	0	0
FR-DE	0.297	0.012	0	0	0	0	0	0

Table 12: Performance of strategy for one calendar year. Total profit (in million €), total volume traded (in million MWh), profit in €/MWh, cost in €/MWh, and average percentage of ATC breaches. Scenario $K = 1$ corresponds to the case discussed at the beginning of Section 5. The ATC breaches are computed as the average (over all 24 contracts) of the number of occurrences when the optimal quantity to trade exceeds the ATC at least once in a day over the number of simulations times 365.

In this subsection we show the performance of the optimal strategy when the investor pays for the use of the interconnector and pays exchange fees. As above, we run 1,000 simulations and compute the terminal average profit for the strategy. Recall that the costs of using the interconnector and exchange fees are given by the diagonal entries in the matrix $\boldsymbol{\Upsilon_2}$ (see Subsection 3.2). Here we assume that $\boldsymbol{\Upsilon_2} = (K-1)\,\boldsymbol{\Upsilon_1}$ where K is a scalar, and recall that $\boldsymbol{\Upsilon_1}$ is the 3×3 diagonal matrix of temporary impact parameters with all entries equal to 0.02. Table 12 reports the total profit, total MWh traded, profit per MWh, cost per MWh, and average

percentage of ATC breaches at $T = 365$ for $K \in \{1, 2, 3, 4, 5, 10, 15, 20\}$. Note that the border DE-CH is the only one to report a relevant percentage of ATC breaches. This is unsurprising, given the relative lower ATC for this trading direction (see Table 2). Observe that as interconnector costs and as exchange fees increase, the strategy finds fewer opportunities to trade and profits decrease. Note that the costs per MWh decrease as the cost factor K increases because costs (temporary impact, interconnector costs, and exchange fees) are quadratic in the speed of trading.

6 Conclusions

We developed a cross-border trading strategy for an agent who trades power among countries that are linked by a power network. Flows of electricity in the European power network were employed to show the effect of imports and exports of power on the prices of the interconnected locations. We find that the price effect of flows of power are direct and indirect. The direct effect results from the import and export of electricity between the two interconnected locations – flows exert an upward pressure on the prices of countries that export (import) power. The indirect price impact results from the knock-on effect that changes in the supply and demand in two countries have on the supply and demand of power of other countries in the network.

The optimal trading strategy and the value function of the agent were obtained in closed-form. We employed transaction data to estimate the model parameters and used simulations to illustrate the performance of the model. The agent imports and exports electricity in France, Germany, and Switzerland. In the extreme case where interconnector costs and exchange fees are zero, we find that the yearly average profit of the strategy is €130 million and the strategy trades an average of 295 million MWh. Clearly, the profits decline when interconnector costs and exchange fees are introduced and when transmission capacity constraints are implemented. For example, when interconnector costs and exchange fees are the same as the costs that stem from the temporary price impact of the trades, profits decrease to €57 million and the strategy trades an average of 130 million MWh.

This paper opens several directions for further research. For example, it could be interesting to study the temporary direct and indirect price impact of cross-border trading more in detail with a fully blown econometric model. The model could also include limit order books information. The network effect we document could also be valid for price volatilities, see e.g.,

Kiesel and Kusterman (2016). Finally, the theoretical framework presented in this paper can be applied in the general context of 'pairs trading' of cross-listed assets.

7 Acknowledgements

M. Flora is grateful to the Mathematical Institute, University of Oxford, for their hospitality and generosity during her visit as a doctoral student to undertake this work. We are grateful to the Department of Economics of the University of Verona for supporting this research through their server infrastructure. T. Vargiolu acknowledges financial support from the research projects of the University of Padova BIRD172407-2017 "New perspectives in stochastic methods for finance and energy markets" and BIRD190200/19 "Term Structure Dynamics in Interest Rate and Energy Markets: Modelling and Numerics". The authors also wish to thank M. Caporin, P. Falbo, A. Ferrante, M. Gallana, P. Morganti, R. Renò, E. I. Ronn, W. Runggaldier, L. Sánchez-Betancourt, and seminar participants at the University of Padova, University of Verona, J.P. Morgan Center for Commodities 4^{th} Annual International Commodities Symposium in Denver, ICIAM 2019 in Valencia, SIAM FM19 in Toronto, EURO18 in Valencia, EFC17 in Krakow, the Stochastics and Optimization in Energy Workshop in London, and the CEMA Conference in Rome. This paper is the recipient of the Best Paper Prize awarded by The Commodity & Energy Markets Association (CEMA) in 2018.

A Appendix

A.1 Econometric analysis results

Here we collect various tables of results of the various econometric analysis we implement.

Table 13: Stepwise OLS robust estimates. Constrained case (4.2). Dependent variable: ΔP_t^F. Explanatory variables: $\mathrm{V}_{t-1}^{SF} - \mathrm{V}_{t-1}^{FS}$ (1), $\mathrm{V}_{t-1}^{GS} - \mathrm{V}_{t-1}^{SG}$ (2), $\mathrm{V}_{t-1}^{GF} - \mathrm{V}_{t-1}^{FG}$ (3), $\mathrm{V}_{t-1}^{GO} - \mathrm{V}_{t-1}^{OG}$ (4), $\mathrm{V}_{t-1}^{FO} - \mathrm{V}_{t-1}^{OF}$ (5), $\mathrm{V}_{t-1}^{SO} - \mathrm{V}_{t-1}^{OS}$ (6).

	01:00	02:00	03:00	04:00	05:00	06:00	07:00	08:00
(1)	0	0	-0.0005^{**}	0	-0.0008^{***}	0	-0.0014^{***}	0
(2)	0	-0.0016^{*}	0.0020^{***}	-0.0011^{**}	0	0	0	0
(3)	0.0003^{*}	0.0020^{***}	0.0011^{***}	0	0.0010^{***}	0	0	0.0018^{***}
(4)	0	0	0.0006^{***}	0	0	0	0	0
(5)	0	0	0	0.0006^{***}	-0.0003^{*}	0	0	-0.0012^{**}
(6)	0	0	0	0	0	0	0	0
	09:00	10:00	11:00	12:00	13:00	14:00	15:00	16:00
(1)	-0.0042^{***}	-0.0025^{***}	-0.0011^{***}	-0.0013^{***}	-0.0019^{***}	-0.0021^{***}	-0.0017^{***}	-0.0017^{***}
(2)	-0.0023^{**}	0	0	0	0	0	0	0
(3)	0	0	0.0011^{**}	0	0.0004^{*}	0	0.0005^{**}	0.0005^{***}
(4)	0	-0.0014^{***}	0	0	0	0	0.0005^{**}	0
(5)	0.0049^{***}	0	0	0.0007^{*}	0	0	0.0008^{*}	0
(6)	0	0	0	0	0	0	0	0
	17:00	18:00	19:00	20:00	21:00	22:00	23:00	24:00
(1)	-0.0025^{***}	-0.0017^{***}	-0.0067^{***}	-0.0031^{***}	-0.0020^{***}	-0.0008^{***}	-0.0009^{***}	-0.0011^{***}
(2)	0	0	0	0	0	0	0	0.0008^{**}
(3)	0.0007^{***}	0.0005^{***}	0	0.0010^{**}	0.0009^{***}	0.0003^{***}	0.0003^{**}	0.0006^{***}
(4)	0.0006^{***}	0	0.0009^{*}	0	0	0	0	0
(5)	0.0010^{***}	0.0018^{***}	0.0019^{**}	0	0	0.0007^{***}	0.0007^{***}	0.0003^{**}
(6)	0	0	0	0	0	0	0	0

Notation: $^{***} = p < 0.01$, $^{**} = p < 0.05$, $^{*} = p < 0.1$.

Table 14: Stepwise OLS robust estimates. Constrained case (4.2). Dependent variable: ΔP_t^S. Explanatory variables: $\mathrm{V}_{t-1}^{SF} - \mathrm{V}_{t-1}^{FS}$ (1), $\mathrm{V}_{t-1}^{GS} - \mathrm{V}_{t-1}^{SG}$ (2), $\mathrm{V}_{t-1}^{GF} - \mathrm{V}_{t-1}^{FG}$ (3), $\mathrm{V}_{t-1}^{GO} - \mathrm{V}_{t-1}^{OG}$ (4), $\mathrm{V}_{t-1}^{FO} - \mathrm{V}_{t-1}^{OF}$ (5), $\mathrm{V}_{t-1}^{SO} - \mathrm{V}_{t-1}^{OS}$ (6).

	01:00	02:00	03:00	04:00	05:00	06:00	07:00	08:00
(1)	0	0	0	0.0004^{***}	0.0007^{***}	0	0.0021^{***}	0.0004^{**}
(2)	-0.0012^{***}	0	0.0012^{***}	0	0	0	0.0020^{***}	0.0011^{*}
(3)	0	0	0	0	0	0	0.0005^{***}	0
(4)	0	0	0	0	0	0	0	0
(5)	0.0012^{***}	0	0	0	0	0	0	-0.0006^{**}
(6)	0	0	0	0	0	0	0	0
	09:00	10:00	11:00	12:00	13:00	14:00	15:00	16:00
(1)	0.0021^{***}	0.0012^{**}	0.0022^{***}	0.0006^{*}	0.0011^{***}	0.0015^{***}	0.0007^{***}	0.0004^{***}
(2)	-0.0008^{**}	0.0102^{***}	0.0035^{**}	-0.0029^{**}	-0.0017^{**}	0.0016^{*}	0	-0.0031^{***}
(3)	0	0	0	0	0.0006^{*}	0	0	0
(4)	0.0002^{*}	0	0	0.0010^{***}	0.0007^{***}	0.0005^{**}	0	0
(5)	0	0	0	0	0	0	-0.0004^{*}	0.0006^{**}
(6)	0	0	0	0	0	0	0	0
	17:00	18:00	19:00	20:00	21:00	22:00	23:00	24:00
(1)	0	0.0018^{***}	0.0012^{***}	0.0007^{***}	0	0.0003^{***}	0.0002^{**}	0.0004^{***}
(2)	0	0	0.0015^{*}	0.0015^{***}	0	-0.0004^{*}	0.0007^{**}	0
(3)	0.0004^{***}	0.0005^{***}	0.0008^{***}	0	0	0	-0.0004^{***}	0
(4)	0.0005^{***}	0	0	0.0002^{**}	0	0	0.0003^{***}	0
(5)	0	0	0.0015^{***}	0	0	0	0	0
(6)	0	0	0	0	0	0	0	0

Notation: $^{***} = p < 0.01$, $^{**} = p < 0.05$, $^{*} = p < 0.1$.

Table 15: Stepwise OLS robust estimates. Constrained case (4.2). Dependent variable: ΔP_t^G. Explanatory variables: $\mathrm{V}_{t-1}^{SF} - \mathrm{V}_{t-1}^{FS}$ (1), $\mathrm{V}_{t-1}^{GS} - \mathrm{V}_{t-1}^{SG}$ (2), $\mathrm{V}_{t-1}^{GF} - \mathrm{V}_{t-1}^{FG}$ (3), $\mathrm{V}_{t-1}^{GO} - \mathrm{V}_{t-1}^{OG}$ (4), $\mathrm{V}_{t-1}^{FO} - \mathrm{V}_{t-1}^{OF}$ (5), $\mathrm{V}_{t-1}^{SO} - \mathrm{V}_{t-1}^{OS}$ (6).

	01:00	02:00	03:00	04:00	05:00	06:00	07:00	08:00
(1)	0.0016^{*}	0	0	0	-0.0025^{*}	0	0	-0.0015^{*}
(2)	0	-0.0042^{**}	-0.0080^{**}	-0.0053^{*}	0	0	0.0067^{*}	-0.0063^{*}
(3)	0	0.0014^{*}	0	0	0	0	-0.0015^{**}	-0.0033^{***}
(4)	0	0	0.0033^{***}	0.0026^{***}	0.0023^{***}	0.0012^{*}	0.0028^{***}	0
(5)	0	0	0	0	0	0	-0.0036^{**}	0
(6)	0	0	0	0	0	0	0	0
	09:00	10:00	11:00	12:00	13:00	14:00	15:00	16:00
(1)	0	0	0	0	0	0	0	0
(2)	0	0	-0.0061^{**}	0	0	0	-0.0040^{**}	0
(3)	0	0	0	0	0	-0.0010^{*}	-0.0017^{***}	-0.0010^{**}
(4)	0	0	0.0021^{***}	0.0026^{***}	0.0031^{***}	0.0029^{***}	0.0033^{***}	0.0032^{***}
(5)	0	0	0	0	0	0	0	0
(6)	0	0	0	0	0	0	0	0
	17:00	18:00	19:00	20:00	21:00	22:00	23:00	24:00
(1)	-0.0009^{*}	-0.0015^{**}	-0.0013^{**}	0	0	0	0	0
(2)	0	0	0	-0.0045^{**}	-0.0034^{**}	0	0	0
(3)	-0.0009^{*}	0	-0.0011^{**}	0	0	0	0	0
(4)	0.0017^{***}	0.0029^{***}	0.0038^{***}	0.0031^{***}	0.0023^{***}	0.0013^{***}	0.0017^{***}	0.0012^{**}
(5)	0	0	0	0	0	0	0	-0.0016^{*}
(6)	0	0	0	0	0	0	0	0

Notation: $^{***} = p < 0.01$, $^{**} = p < 0.05$, $^{*} = p < 0.1$.

A.2 Proofs

A.2.1 Proof of Prop. 3.1

The supremum in (3.11) attains a maximum because it is quadratic and negative definite in $\boldsymbol{\nu}$ as the values of the temporary price impact parameters are positive. It is straightforward to obtain the first order condition for the vector of controls $\boldsymbol{\nu}$ and (3.14) follows by direct substitution.

A.2.2 Proof of Prop. 3.2

Differentiate (3.16) and because we assume that the matrix $\boldsymbol{E}(t)$ is symmetric, we have

$$V_t = A'(t) + \boldsymbol{D}'^{\intercal}(t)\,\mathbf{P} + \boldsymbol{P}^{\intercal}\,\boldsymbol{E}'(t)\,\mathbf{P}, \qquad V_P = 2\,\boldsymbol{E}(t)\,\mathbf{P}, \qquad V_{PP} = 2\,\boldsymbol{E}(t)\,. \tag{A.1}$$

Insert the expressions for V_P and V_{PP} into the PIDE (3.14) and write

$$\begin{aligned} A'(t) + \boldsymbol{D}'^{\intercal}(t)\,\mathbf{P} + \mathbf{P}^{\intercal}\,\boldsymbol{E}'(t)\,\mathbf{P} + \mathcal{L}^{\mathbf{0}}\,V(t,\mathbf{P}) + \tfrac{1}{4}\,\{\,\boldsymbol{H}^{\intercal}\,[\,\boldsymbol{D}(t) + 2\boldsymbol{E}(t)\,\mathbf{P}\,] + \boldsymbol{B}^{\intercal}\,\mathbf{P} + \boldsymbol{\Theta}(t)\,\}^{\intercal}\,\boldsymbol{\Upsilon}^{-1} \\ \times\,\{\,\boldsymbol{H}^{\intercal}\,(\,\boldsymbol{D}(t) + 2\boldsymbol{E}(t)\,\mathbf{P}\,) + \boldsymbol{B}^{\intercal}\,\mathbf{P} + \boldsymbol{\Theta}(t)\,\} = 0\,, \end{aligned} \tag{A.2}$$

where $\mathcal{L}^{\mathbf{0}}$ is the infinitesimal generator obtained under the null control. For the jump part we have

$$V(t,\mathbf{P} + y\,\mathbb{1}_i) = A(t) + \boldsymbol{D}^{\intercal}(t)\,\mathbf{P} + D_i(t)\,y + \mathbf{P}^{\intercal}\,\boldsymbol{E}(t)\,\mathbf{P}\,y\,\mathbb{1}_i^{\intercal}\,\boldsymbol{E}(t)\,\mathbf{P} + \mathbf{P}^{\intercal}\,\boldsymbol{E}(t)\,y\,\mathbb{1}_i + y^2\,\mathbb{1}_i^{\intercal}\,\boldsymbol{E}(t)\,\mathbb{1}_i\,,$$

and

$$(\Delta_i(y)\,V)(t,\mathbf{P}) = D_i(t)\,y + 2\sum_{j=1}^{n} P_j\,E_{ij}(t)\,y + E_{ii}(t)\,y^2\,, \tag{A.3}$$

where the last step follows because we assume $\boldsymbol{E}(t)$ is symmetric. Thus,

$$\begin{aligned} &\sum_{i=1}^{n}\lambda_i\int_{-\infty}^{+\infty}(\Delta_i(y)\,V)(t,\mathbf{P})\,\frac{1}{\sqrt{2\,\pi}\,\xi_i}\,\mathrm{e}^{\frac{-(y-\psi_i)^2}{2\,\xi_i^2}}\,\mathrm{d}y \\ &\quad = \sum_{i=1}^{n}\lambda_i\left[\left(D_i(t) + 2\sum_{j=1}^{n}P_j\,E_{ij}(t)\right)\,\psi_i + E_{ii}(t)\,\left(\xi_i^2 + \psi_i^2\right)\right]\,, \end{aligned} \tag{A.4}$$

where the last step follows from properties of Gaussian distributions. Finally, we obtain

$$\int_{-\infty}^{+\infty} J\,\Delta V(t,\mathbf{P})\,\mathrm{d}y = [\,\boldsymbol{D}^{\intercal}(t) + 2\,\mathbf{P}^{\intercal}\,\boldsymbol{E}(t)\,]\,(\,\boldsymbol{\lambda}\circ\boldsymbol{\psi}\,) + \boldsymbol{\psi}^{\intercal}\,diag(\boldsymbol{E}(t))\,(\,\boldsymbol{\lambda}\circ\boldsymbol{\psi}\,) + \boldsymbol{\xi}^{\intercal}\,diag(\boldsymbol{E}(t))\,(\,\boldsymbol{\lambda}\circ\boldsymbol{\xi}\,)\ . \tag{A.5}$$

Now, collect quadratic terms of $\mathbf{P}$ in (A.2) and write

$$\begin{aligned} 0 = {} & \boldsymbol{E}'(t) + \tfrac{1}{2}\,\boldsymbol{E}^{\intercal}(t)\,\boldsymbol{H}\,\boldsymbol{\Upsilon}^{-1}\,\boldsymbol{B}^{\intercal} + \left(\tfrac{1}{2}\,\boldsymbol{H}\,\boldsymbol{\Upsilon}^{-1}\,\boldsymbol{B}^{\intercal}\right)^{\intercal}\boldsymbol{E}(t) - \boldsymbol{\Phi}^{\intercal}\,\boldsymbol{E}(t) - \boldsymbol{\Phi}^{\intercal}\,\boldsymbol{E}(t) \\ & + \boldsymbol{E}^{\intercal}(t)\,\boldsymbol{H}\,\boldsymbol{\Upsilon}^{-1}\,\boldsymbol{H}^{\intercal}\,\boldsymbol{E}(t) + \tfrac{1}{4}\,\boldsymbol{B}\,\boldsymbol{\Upsilon}^{-1}\,\boldsymbol{B}^{\intercal} \end{aligned} \tag{A.6}$$

to obtain Equation (3.17). Collect linear terms in (A.2) and write

$$0 = \boldsymbol{D}'(t) + \boldsymbol{E}^{\intercal}(t)\,\boldsymbol{H}\,\boldsymbol{\Upsilon}^{-1}\,(\,\boldsymbol{H}^{\intercal}\,\boldsymbol{D}(t) + \boldsymbol{\Theta}(t)\,) + \tfrac{1}{2}\,\boldsymbol{B}\,\boldsymbol{\Upsilon}^{-1}\,\,(\,\boldsymbol{H}^{\intercal}\,\boldsymbol{D}(t) + \boldsymbol{\Theta}(t)\,) + 2\,\boldsymbol{E}(t)(\,\boldsymbol{\theta} + \boldsymbol{\lambda}\circ\boldsymbol{\psi}\,) - \boldsymbol{\Phi}^{\intercal}\,\boldsymbol{D}\,,$$

which results in (3.18). Finally, collect constant terms to obtain (3.19), with terminal condition $A(T) = \boldsymbol{D}(T) = \boldsymbol{E}(T) = 0$.

A.3 Verification

In this section we verify that the solution we obtained above is indeed the value function in (3.10) of the agent and that the optimal speed of trading is an admissible control. First, we need a technical lemma.

Lemma A.1. *For all $\boldsymbol{\nu} \in \mathcal{A}$, for all $t \in [0,T]$ and for all initial conditions $\mathbf{P} \in \mathbb{R}^n$, the process $\boldsymbol{P}^{\boldsymbol{\nu};t,\mathbf{P}}$ is such that*

$$\mathbb{E}_{t,\mathbf{P}}\left[\sup_{t\le u\le T}\left\|\boldsymbol{P}_u^{\boldsymbol{\nu};t,\mathbf{P}}\right\|^2\right] < \infty\,.$$

Proof. For $u \in [t,T]$, the SDE for the price process (3.2) has the unique solution

$$\begin{aligned} \boldsymbol{P}_u^{\boldsymbol{\nu};t,\mathbf{P}} &= e^{-(u-t)\,\boldsymbol{\Phi}}\,\boldsymbol{P}_t + \int_t^u e^{-(v-t)\,\boldsymbol{\Phi}}\,(\boldsymbol{\theta} + \boldsymbol{H}\,\boldsymbol{\nu}_v)\,\mathrm{d}v + \int_t^u e^{-(v-t)\,\boldsymbol{\Phi}}\,(\boldsymbol{\sigma}\,\mathrm{d}\mathbf{W}_t + J(\boldsymbol{\psi},\boldsymbol{\xi})\,\mathrm{d}\boldsymbol{\Pi}(\boldsymbol{\lambda})) \\ &= \boldsymbol{P}_u^{0;t,\mathbf{P}} + \int_t^u e^{-(v-t)\,\Phi}\,\boldsymbol{H}\,\boldsymbol{\nu}_v\,\mathrm{d}v\,. \end{aligned}$$

Thus,

$$\mathbb{E}_{t,\mathbf{P}}\left[\sup_{t\le u\le T}\|\boldsymbol{P}_u^{\boldsymbol{\nu}}\|^2\right] \le 2\,\mathbb{E}_{t,\mathbf{P}}\left[\sup_{t\le u\le T}\|\boldsymbol{P}_u^{\mathbf{0}}\|^2\right] + 2\,\mathbb{E}_{t,\mathbf{P}}\left[\sup_{t\le u\le T}\left\|\int_t^u e^{-(v-t)\,\boldsymbol{\Phi}}\,\boldsymbol{H}\,\boldsymbol{\nu}_v\,\mathrm{d}v\right\|^2\right]\,.$$

The first term on the right-hand side is finite because the process $\mathbf{P}^{\mathbf{0};t,\mathbf{P}}$ is a solution of (3.2), with the control set to zero, that satisfies the assumptions of Protter (2003, Theorem V.67) while the second term obeys the bounds:

$$\begin{aligned}\mathbb{E}_{t,\mathbf{P}}\left[\sup_{t\le u\le T}\left\|\int_t^u e^{-(v-t)\,\boldsymbol{\Phi}}\,\boldsymbol{H}\,\boldsymbol{\nu}_v\,\mathrm{d}v\right\|^2\right] &\le \mathbb{E}_{t,\mathbf{P}}\left[\int_t^T \|e^{-(v-t)\,\boldsymbol{\Phi}}\,\boldsymbol{H}\|^2\|\boldsymbol{\nu}_v\|^2\,\mathrm{d}v\right]\\ &\le \sup_{t\le v\le T}\|e^{-(v-t)\,\boldsymbol{\Phi}}\,\boldsymbol{H}\|^2\,\mathbb{E}_{t,\mathbf{P}}\left[\int_t^T\|\boldsymbol{\nu}_v\|^2\,\mathrm{d}v\right],\end{aligned}$$

which is finite because $[t,T]\ni v\to e^{-(v-t)\,\boldsymbol{\Phi}}\,\boldsymbol{H}$ is continuous and bounded, and $\boldsymbol{\nu}$ is admissible.

□

Theorem A.1 (Verification Theorem)**.** *Assume that for a certain $t\in[0,T]$ the matrix-valued function $t\to\boldsymbol{E}(t)$, defined in* (3.22)*, is the unique C^0 solution of* (A.6) *on $[t,T]$. Then, the function V in* (3.16)*, which is a solution of the HJB* (3.11)*, coincides with the value function* (3.10)*, and the process $\boldsymbol{\nu}^*$ defined in* (3.13) *is the optimal control for the problem in* (3.10)*.*

Proof. The proof is based on the general result in Fleming and Soner (1993, Theorem III.8.1). We know that V is a classical (i.e., $C^{1,2}$) solution of the HJB (3.11). Thus, it follows that $V(t,\mathbf{P})\ge Z(t,\boldsymbol{P};\boldsymbol{\nu})\ \forall\ \boldsymbol{\nu}\in\mathcal{A}$, provided that the Dynkyn formula

$$\mathbb{E}_{t,\boldsymbol{P}}[V(T,\boldsymbol{P}_T)] = V(t,\mathbf{P}) + \mathbb{E}_{t,\boldsymbol{P}}\left[\int_t^T \mathcal{L}^{\boldsymbol{\nu}}V(u,\boldsymbol{P}_u)\,\mathrm{d}u\right] \tag{A.7}$$

holds. To prove this, first note that, for a suitable constant c,

$$|\mathcal{L}^{\boldsymbol{\nu}}V(u,\mathbf{P})|\le c\,\left(1+\|\mathbf{P}\|^2+\|\mathbf{P}\|\,\|\boldsymbol{\nu}\|\right),$$

because V is bilinear in $\mathbf{P}$. This, together with Lemma A.1 and the admissibility of $\boldsymbol{\nu}$, gives that the integral on the right-hand side of (A.7) is well defined.

To prove Dynkyn's formula (A.7), we first apply Itō's formula to $V(t,\boldsymbol{P}_t^{\boldsymbol{\nu}})$ and write

$$V(T,\boldsymbol{P}_T^{\boldsymbol{\nu}}) = V(t,\mathbf{P}) + I_T^1 + I_T^2 + \int_t^T \mathcal{L}^{\boldsymbol{\nu}}V(u,\boldsymbol{P}_u^{\boldsymbol{\nu}})\,\mathrm{d}u\,, \tag{A.8}$$

where the processes $(I_u^1)_{u\in[t,T]}$ and $(I_u^2)_{u\in[t,T]}$ are given by

$$\begin{aligned} I_u^1 &= \int_t^u (\boldsymbol{D}(v) + 2\,\boldsymbol{E}(v)\,\boldsymbol{P}_v^{\boldsymbol{\nu}})^\intercal\,\boldsymbol{\sigma}\,\mathrm{d}\boldsymbol{W}_v\,, \\ I_u^2 &= \int_t^u (\boldsymbol{D}(v) + 2\,\boldsymbol{E}(v)\,\boldsymbol{P}_{v-}^{\boldsymbol{\nu}})^\intercal\,J(\boldsymbol{\psi},\boldsymbol{\xi})\,\mathrm{d}\boldsymbol{\Pi}(\boldsymbol{\lambda})\,. \end{aligned}$$

By Itō's isometry and arguments similar to those of Lemma A.1, the process I^1 is a martingale. For the process I^2, we check for all $u \in [t,T]$ the finiteness of

$$\begin{aligned} \mathbb{E}_{t,\mathbf{P}}\left[\left\|\int_t^u J(\boldsymbol{\psi},\boldsymbol{\xi})\;\mathrm{d}\boldsymbol{\Pi}(\boldsymbol{\lambda})\right\|^2\right] &= \sum_{k=1}^n \mathbb{E}_{t,\mathbf{P}}\left[\left(\sum_{\ell=1}^{\Pi_u^k} J_\ell^k\right)^2\right] \\ &= \sum_{k=1}^n \mathbb{E}_{t,\mathbf{P}}\left[\Pi_u^k\,(\psi_k^2+\xi_k^2)\right] = \sum_{k=1}^n \lambda_k\,(u-t)\,(\psi_k^2+\xi_k^2) < \infty\,, \end{aligned}$$

see Protter (2003, Theorem V.66).

Next, note that $v \to \big(\boldsymbol{D}(v) + 2\,\boldsymbol{E}(v)\,\boldsymbol{P}_{v-}^{\boldsymbol{\nu}}\big)^\intercal$ is predictable because it is left-continuous, thus (see Protter (2003, Theorem V.66)) there exists a constant $m > 0$ such that

$$\mathbb{E}_{t,\mathbf{P}}\left[\sup_{u\in[t,T]} |I_u^2|^2\right] \le m\int_t^T \mathbb{E}_{t,\mathbf{P}}\left[\|\boldsymbol{D}(u) + 2\,\boldsymbol{E}(u)\,\boldsymbol{P}_{u-}^{\boldsymbol{\nu}}\|^2\right]\,\mathrm{d}u\,,$$

where the right-hand side is finite, as shown above for I^1. Hence, the process I^2 is a martingale and we take the expectation of (A.8) to obtain Dynkyn's formula (A.7). Therefore, $V(t,\mathbf{P}) \ge Z(t,\mathbf{P};\boldsymbol{\nu})\ \forall\ \boldsymbol{\nu} \in \mathcal{A}$.

Next we show that the control we found is indeed the optimal control. We have that $\boldsymbol{\nu}^*(t,\mathbf{P})$ defined in (3.13) is a maximiser of the HJB equation (3.11). Thus, we only need to check that the control process $(\boldsymbol{\nu}^*(t,\boldsymbol{P}_t))_t \in \mathcal{A}$. The control process is progressively measurable by construction, so we only need to check that it is square integrable; however, because $\boldsymbol{\nu}^*$ is linear in $\boldsymbol{P}$ and Lemma A.1, we have that $\mathbb{E}_{t,\mathbf{P}}\left[\int_t^T \|\boldsymbol{\nu}^*(u,\boldsymbol{P}_u)\|^2\,\mathrm{d}u\right] < \infty$ and $(\boldsymbol{\nu}^*(t,\boldsymbol{P}_t))_t \in \mathcal{A}$, as required. □

References

Alfonsi, A., Fruth, A., Schied, A. (2010) *Optimal execution strategies in limit order books with general shape functions.* Quantitative Finance, vol. 10(2): 143-157.

Benth, F. E., Kallsen, J., Meyer-Brandis, T. (2007) *A non-Gaussian Ornstein-Uhlenbeck process for electricity spot price modeling and derivatives pricing.* Applied Mathematical Finance 14(2): 153-169.

Benth, F. E., Kiesel, R., and Nazarova, A. (2012). *A critical empirical study of three electricity spot price models.* Energy Economics, 34 (5): 1589–1616.

Bini, D. A., Iannazzo, B., Meini, B. (2012) *Numerical solution of algebraic Riccati equations.* Society for Industrial and Applied Mathematics Philadelphia, PA, USA.

Borak, S., Weron, R. (2008) *A semiparametric factor model for electricity forward curve dynamics.* Journal of Energy Markets 1(3): 3-16.

Cartea, Á., Figueroa, M.G. (2005) *Pricing in Electricity Markets: a mean reverting jump diffusion model with seasonality.* Applied Mathematical Finance, 12(4): 313-335.

Cartea, Á., Figueroa, M.G., Geman, H. (2009) *Modelling Electricity Prices with Forward Looking Capacity Constraints.* Applied Mathematical Finance, 16(2): 103-122.

Cartea, Á., González-Pedraz, C. (2012) *How much should we pay for interconnecting electricity markets? A real options approach.* Energy Economics, 34: 14-30.

Cartea, Á., Jaimungal, S. (2016a) *Algorithmic Trading of Co-Integrated Assets.* International Journal of Theoretical and Applied Finance, vol. 19, issue 6.

Cartea, Á., Jaimungal, S. (2016b) *Incorporating order-flow into optimal execution.* Mathematics and Financial Economics, vol. 10(3): 339-364.

Cartea, Á., Jaimungal, S., Penalva, J. (2015) *Algorithmic and high-frequency trading* (1st ed.) Cambridge: Cambridge University Press.

Cartea, Á., Jaimungal, S., Qin, Z. (2019) *Speculative trading of electricity contracts in interconnected locations.* Energy Economics, 79: 3-20.

Draper, N. R., Smith, H., (1998) *Applied Regression Analysis.* Hoboken, NJ: Wiley-Interscience, 1998. pp. 307–312.

Engle, R., Granger, C. (1987) *Co-integration and error correction: representation, estimation and testing.* Econometrica, 55: 251-276.

Fleming, W., Soner, M. (1993), *Controlled Markov Processes and Viscosity Solutions*. New York: Springer-Verlag.

Geman, H., Roncoroni, A. (2006) *Understanding the fine structure of electricity prices*. The Journal of Business, 79 (3): 1225–1261.

Gianfreda, A., Bunn, D. (2018) *A stochastic latent moment model for electricity price formation*. Operations Research, 66 (5): 1189–1203.

Glas, S., Kiesel, R., Kolkmann, S., Kremer, M., Graf von Luckner, N., Ostmeier, L., Urban, K., Weber, C. (2019) *Intraday renewable electricity trading: Advanced modeling and numerical optimal control*. Working paper.

Gombani, A., Runggaldier, W. J. (2013) *Arbitrage-free multifactor term structure models: a theory based on stochastic control*. Mathematical Finance, 23(4): 659-686.

Hambly, B., Howison, S., Kluge, T. (2009) *Modelling spikes and pricing swing options in electricity markets*. Quantitative Finance, 9(8): 937-949, doi.org/10.1080/14697680802596856.

Kiesel, R., Kusterman, M. (2016) *Structural models for coupled electricity markets*. Journal of Commodity Markets, 3: 16-38.

Kiesel, R., Paraschiv, F., Sætherø, A. (2019) *On the construction of hourly price forward curves for electricity prices*. Computational Management Science, 16: 345-369.

Kiesel, R., Schindlmayr, G., Börger, R. (2009) *A two-factor model for the electricity forward market*. Quantitative Finance, 9(3): 279-287.

Lei, Y., Xu, J. (2015) *Costly arbitrage through pairs trading*. Journal of Economic Dynamics and Control, 56: 1-19.

Leung, T., Li, X. (2015) *Optimal mean reversion trading with transaction costs and stop-loss exit*. International Journal of Theoretical and Applied Finance, 18(03).

Lintilhac, P. S., Tourin, A. (2017) *Model-based pairs trading in the bitcoin markets*. Quantitative Finance, 17(05): 703-716.

Lucia, J. J., Schwartz, E. S. (2002) *Electricity prices and power derivatives: Evidence from the Nordic power exchange*. Review of Derivatives Research, 5: 5-50.

McInerney, C., Bunn, D. (2013) *Valuation anomalies for interconnector transmission rights.* Energy Policy, 55 565-578.

Mudchanatongsuk, S., Primbs, J. A., Wong, W. (2008) *Optimal pairs trading: a stochastic control approach.* American Control Conference, June 11-13 2008: 1035-1039.

Newbery, D., Strbac, G., Viehoff, I. (2016) *The benefits of integrating European electricity markets.* Energy Policy, 94: 253-263.

Øksendal, B., Sulem, A. (2007) *Applied stochastic control of jump diffusions.* 2nd ed., Springer.

Pilipovic, D. (1998) *Energy risk: valuing and managing energy derivatives.* New York: McGraw-Hill.

Protter, P. (2003) *Stochastic Integration and Differential Equations, 2nd edn.* Berlin Heidelberg: Springer.

Roncoroni, A. (2002) *A class of marked point processes for modeling electricity prices.* PhD, Université Paris IX Dauphine.

Ronn, E. I., Wimschulte, J. (2006) *Intra-day risk premia in European electricity forward markets.* Journal of Energy Markets, 2 (4): 71–98.

Seifert, J., Uhrig-Homburg, M. (2007) *Modelling jumps in electricity prices: theory and empirical evidence.* Review of Derivatives Research, 10: 59-85.

Tourin, A., Yan, R. (2013) *Dynamic pairs trading using the stochastic control approach.* Journal of Economic Dynamics and Control, 37(10): 1972-1981.

Vaughan, D. R. (1969) *A negative exponential solution for the matrix Riccati equation.* IEEE Transactions on Automatic Control, 14(1): 72–75.

Weron, R. (2007) *Modeling and forecasting electricity loads and prices: a statistical approach.* Volume 403, John Wiley & Sons.